January 2014

Channel Estimation And Correction Methods For Ofdma Based Lte Downlink System

Zahirul Islam

CHANNEL ESTIMATION AND CORRECTION METHODS FOR OFDMA BASED LTE
DOWNLINK SYSTEM

by

Zahirul Islam

Bachelor of Science, Stamford University Bangladesh, 2008

A Thesis

Submitted to the Graduate Faculty

of the

University of North Dakota

In partial fulfillment of the requirements
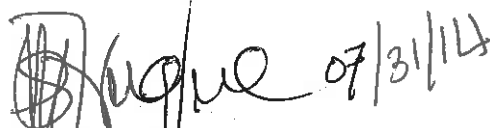

for the degree of

Master of Science

Grand Forks, North Dakota
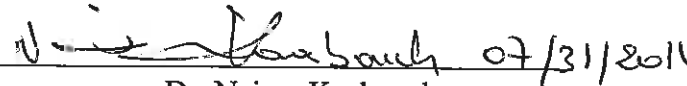
August
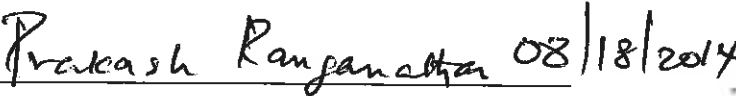
2014

This thesis, submitted by Zahirul Islam in partial fulfillment of the requirements for the Degree of Masters of Science from the University of North Dakota, has been read by the Faculty Advisory Committee under whom the work has been done and is hereby approved.

_____ 07/31/14
Dr. Saleh Faruque, Chair

_____ 07/31/2014
Dr. Naima Kaabouch

_____ 08/18/2014
Dr. Prakash Ranganathan

This thesis meets the standards for appearance, conforms to the style and format requirements of the Graduate School of the University of North Dakota, and is hereby approved.

_____
Wayne Swisher
Dean of the School of Graduate Studies

_____
Date   August 19, 2014

iii

PERMISSION

Tittle   Channel estimation and correction methods for OFDMA based LTE Downlink system

Department Electrical Engineering

Degree   Master of Science

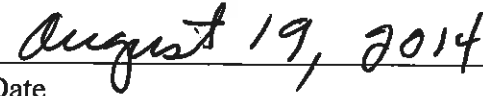In presenting this thesis in partial fulfillment of the requirements for a graduate degree from the University of North Dakota, I agree that the library of this University shall make it freely available for inspection. I further agree that permission for extensive copying for scholarly purposes may be granted by the professor who supervised my thesis work or, in his absence, by the chairperson of the department or the dean of the Graduate School. It is understood that any copying or publication or other use of this thesis or part thereof for financial gain shall not be allowed without my written permission. It is also understood that due recognition shall be given to me and to the University of North Dakota in any scholarly use which may be made of any material in my thesis.

Signature Zahirul Islam

Date 7/31/2014

TABLE OF CONTENTS

LIST OF FIGURES

LIST OF TABLES

LIST OF ACRONYMS

3GPP	3rd Generation Partnership Project
4G	4th generation
A/D	Analog/Digital
BER	Bit Error Rate
CP	Cyclic Prefix
CQI	Channel Quality Indicator
DFT	Discrete Fourier Transform
E-UTRA	Evolved UMTS Terrestrial Radio Access
FDD	Frequency Division Duplex
FDMA	Frequency Division Multiple Access
FFT	Fast Fourier Transform
GSM	Global System for Mobile communications
H-ARQ	Hybrid Automated Repeat Request
ICI	Inter Carrier Interference
ISI	Inter Symbol Interference
INTHFT	Institute of Communications and Radio-Frequency Engineering
IFFT	Inverse Fast Fourier Transform
LS	Least Squares
LTE	Long Term Evolution
LMMSE	Linear Minimum Mean Square Error
MAC	Medium Access Control
MCS	Modulation and Coding Scheme
MIMO	Multiple Input Multiple Output
MSE	Mean Square Error
MU-MIMO	Multi User MIMO
OFDM	Orthogonal Frequency Division Multiplexing
OFDMA	Orthogonal Frequency Division Multiple Access

PAPR	Peak-to-Average Power Ratio
PBCH	Physical Broadcast Channel
PL	Path Loss
PRACH	Physical Random Access Channel
PSS	Primary Synchronization Signal
PDCCH	Physical Downlink Control Channel (PDCCH)
PUCCH	Physical Uplink Control Channel
PUSCH	Physical Uplink Shared Channel
RE	Resource Element
RI	Rank Indicator
QAM	Quadrature Amplitude Modulation
QPSK	Quadrature Phase Shift Keying
RB	Resource Block
RF	Radio Frequency
SINR	Signal to Interference and Noise Ratio
SIR	Signal to Interference Ratio
SISO	Single Input Single Output
SMS	Short Message Service
SNR	Signal to Noise Ratio
SUI	Stanford University Interim
T-F	Time-Frequency
TDMA	Time Division Multiple Access
TTI	Transmission Time Interval
UE	User Equipment
ULSCH	Uplink Shared Channel
WAP	Wireless Application Protocol
WiMAX	Worldwide Inter-operability for Microwave Access
W-CDMA	Wideband Code Division Multiple Access

ACKNOWLEDGEMENTS

To my family.

ABSTRACT

In present era, cellular communication plays a vital role for communicating over long distance. The number of mobile subscribers is increasing tremendously day by day. 3GPP LTE is the evolution of the UMTS in response to ever-increasing demands for high quality multimedia services according to users' expectations. The average data consumption exceeds hundreds of Megabytes per subscriber per month. To introduce, summarize and get acquainted with this new technology LTE is one of the main objectives of my thesis.

The Downlink is always considered an important factor in terms of coverage and capacity aspects in between Downlink and Uplink factors for cellular communication. Orthogonal Frequency Division Multiple Access (OFDMA) and Multiple Input Multiple Output (MIMO) are the new technologies which enhance the performance of the traditional wireless communication experience for downlink. In this thesis, we considered the downlink system for channel estimation by using different algorithms and interpolation methods.

Channel Estimation algorithms such as Least Squares Estimation (LSE) and Minimum Mean Square Error (MMSE) have been evaluated for different channel models. The interpolation method used in algorithms is Linear, Piecewise constant, Averaged and Pilot averaged. I measured the performance of these algorithms in terms of Bit Error Rate (BER) and Symbol Error Rate (SER). The results are presented to illustrate the salient concept of the LTE communication system.

CHAPTER 1

INTRODUCTION

The support for voice and data services has developed enormously in recent years and the demands for higher data rates along with high quality wireless communications has also increased. Limitations in bandwidth resources and immense increase in the number of users become an unavoidable issue to be solved. So, there is a need to improve wireless communications by adopting advanced technologies to use the available spectrum in an efficient way. Orthogonal Frequency Division Multiplexing (OFDM) and Multiple Input Multiple Output (MIMO) systems are examples of technologies which can enhance the performance of the wireless communications systems. These systems can bring the advantages of using high data rates and high quality voice simultaneously. On the other hand, cheaper installation and maintenance cost along with superior performance would be highly desirable. Therefore, Long Term Evolution (LTE) of the Evolved Packet System (EPS) becomes a revolutionary move in the field of mobile communications which can fulfill the demand for high speed connections on networks, low latency and delay and high peak data rates. LTE leverages on a number of technologies namely Multi Input Multiple Output (MIMO) antennas, Orthogonal Frequency Division Multiplexing (OFDM) and Orthogonal Frequency Division Multiplexing Access (OFDMA) at the downlink, Single Carrier Frequency Division Multiple Access (SCFDMA) at the uplink, support for Quadrature Phase Shift Keying (QPSK), 16 Quadrature Amplitude Modulation (16QAM), and 64QAM [1].

1.1   Thesis Outline

Chapter 2 starts with a brief description of evolutions of wireless technology along with the modulation techniques, multiple access schemes and propagation & fading of the communication channel.   After that it also describes the motivation of the thesis and contributions accordingly.

Chapter 3 contains an introduction to LTE physical layer for both downlink and uplink transmission. It also describes the modulation techniques, synchronization, frequency allocation and channel structure for downlink and uplink transmission.

Chapter 4 contains a brief overview of available channel estimation methods and related results as literature review.

Chapter 5 represents the simulation and results of the available channel estimation methods for OFDMA based downlink systems. The analysis mainly based on MATLAB simulation (LTE PHY Lab) [2].

Chapter 6 presents the conclusions and outlooks future work of the thesis work based on simulations and experimental result analysis.

CHAPTER 2

BACKGROUND

The concept of wireless communications is considered one of the greatest achievements of all time. It was first introduced by Guglielmo Marconi in 1897. It is widely used in broadcasting of television, radio, satellite transmission and cellular networks in today's world. In between them, cellular communications has experienced significant development within the last two decades.

Table 1 shows the evolution of wireless technology briefly elaborated from 2G to 4G according to the corresponding multiple access techniques, frequency bands and throughputs.

The evolution of mobile standards

Mobile standards	3GPP		Qualcomm	China	IEEE
Carriers using:	AT&T and T-Mobile US, majority of global carriers		Sprint, Verizon Wireless	China Mobile	Sprint
2G: digital + data services	GSM: 2G		CDMAOne		
	GPRS: 2.5G				
	EDGE: 2.75G				
3G: at least 200 kbps iPhone 4 currently delivers up to 7.2Mbps down, 5.8Mbps up	Release 4	UMTS 3G	CDMA2000 EVDO rev 0	TD-SCDMA (up to 2Mbps)	
	Release 5	HSDPA 3.5G (to 21 Mbps down)	CDMA2000 EVDO rev A (up to 3.1 Mbps down, 1.8 up)		
	Release 6	HSUPA 3.5G (to 5.8Mbps up)	EVDO Rev C / Ultra Mobile Broadband Canceled: Sprint moving to WiMAX, Verizon moving to 3GPP LTE		Mobile WiMAX 3.9G (4 Mbps cap on EVO "4G")
	Release 7	HSPA+ 3.5G			
	Release 8/9	LTE 3.9G			
4G: at least 100 Mbps, IP-based	Release 10	LTE Advanced		TD-LTE	WiMAX 4G

Table 1: Wireless Technology Evolution [3]

2.1   Communication Model

In general, there are three main parts of a communication model. (Figure 1)

1) Transmitter: It transmits the information or data from the source to the channel.

2) Channel: It is a medium where transmitter can transmit the signal to the receiver. The quality

of the signal is greatly depends on the channel strength and distance.

3) Receiver: It receives the signal from the channel and recovers the information signal from

transmission loss due to attenuation and interference.
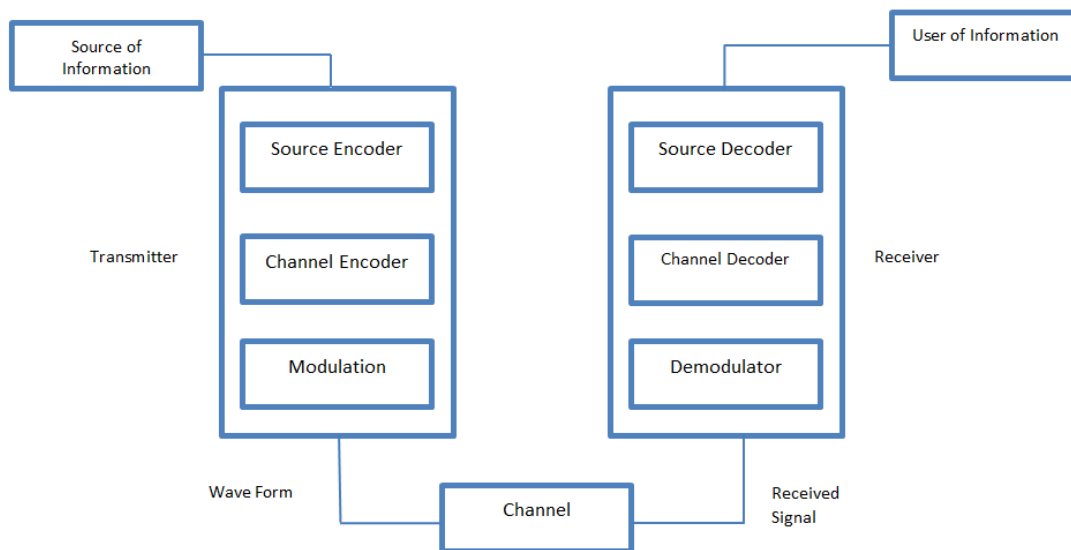
Figure 1: Basic Communication Model

The modulator and demodulator play a vital role in communication systems. At the

transmitter side, the information signal is modulated by carrier frequency. After getting the

carrier frequency added information from channel, it is removed from the information signal at

the receiver side to retrieve the original signal [4].

2.2   Multiple Access Schemes

Multiple Accesses allow users to share the same channel on the basis of frequency, time, space and code [5]. The well known multiple access schemes include:

1) Time Division Multiple Access (TDMA)

2) Code Division Multiple Access (CDMA)

3) Frequency Division Multiple Access (FDMA)

4) Space Division Multiple Access (SDMA)

5) Orthogonal Frequency Division Multiple Access (OFDMA)

6) Single Carrier Frequency Division Multiple Access (SC-FDMA)

2.2.1 Time Division Multiple Access (TDMA)

TDMA is mainly based on time-division multiplexing (TDM) scheme, which provides different time-slots to different data –streams in a cyclically repetitive frame structure. Several users access the same frequency channel for different time slots and each user is assigned a separate time slot for a specific period that transmits signal in rapid succession. It is used in GSM, IS-136, PDC and iDEN.

2.2.2 Frequency Division Multiple Access (FDMA)

FDMA is based on frequency-division multiplexing (FDM) scheme, which provides different frequency bands to different data streams. One channel is assigned to one user for entire call duration which is not an efficient scheme. FDMA is used in 1G (AMPS).

2.2.3 Code Division Multiple Access (CDMA)

In this system, the data is transmitted over the entire frequency range available. CDMA is a form of multiplexing system. It allows a number of signals to occupy a signle transmission channel which optimize the available bandwidth. It is used by 2G and 3G wireless communications and typically operates in the frequency range of 800 MHz to 1.9 MHz. With the combination with spread spectrum technology, CDMA employs analog-to-digital conversion (ADC).

Figure 2 shows a basic frequency vs time diagram of FDMA, TDMA and CDMA.
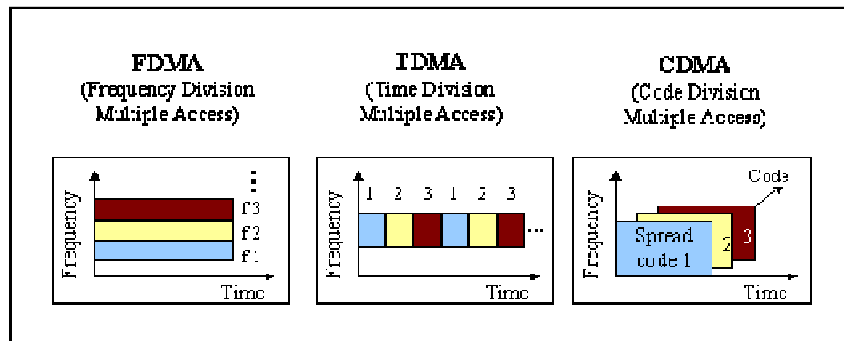
Figure 2: Comparison between FDMA, TDMA & CDMA [6]

2.2.4 Orthogonal Frequency Division Multiplexing Access (OFDMA)

In OFDM systems, the available bandwidth is broken into many narrower subcarriers [7]. The data is divided into parallel streams, one for each subcarrier each of is then modulated using varying levels of QAM modulation e.g. QPSK, 16QAM, 64QAM or higher orders as required by the desired signal quality.

Figure 2 shows a basic block diagram of OFDMA transmitter and receiver. In the transmitter end, bits are modulated in the modulator and then become serial to parallel. Each of

the OFDM symbol is preceded by a cyclic prefix (CP) which is effectively used to eliminate Intersymbol Interference (ISI). The subcarriers are also very tightly spaced for efficient utilization of the available bandwidth.
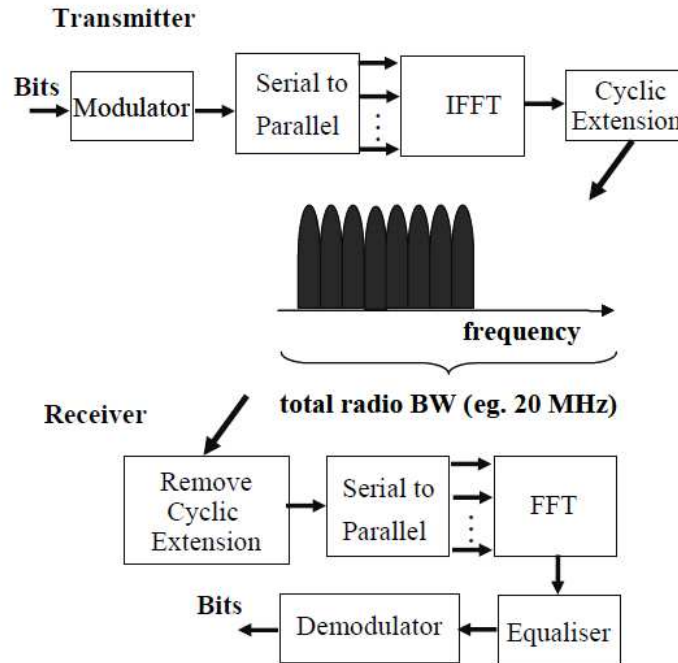
Figure 3: OFDMA transmitter and receiver [8]

2.2.5 Single Carrier – Frequency Division Multiple Access (SC-FDMA)

A SC-FDMA signal can be generated by using the discrete fourier transform (DFT) - spread OFDM digital signal processing. The data symbols are spread over all the subcarriers carrying information and produce a virtual single-carrier structure [9].

Figure 4 shows a comparison between a frequency domain SC-FDMA and OFDMA. SC-FDMA has lower PAPR compare to OFDM. In SC-FDMA, the bandwidth is divided into

multiple parallel subcarriers with cyclic prefix in the time domain in order to stay orthogonal to each other and eliminate ISI.
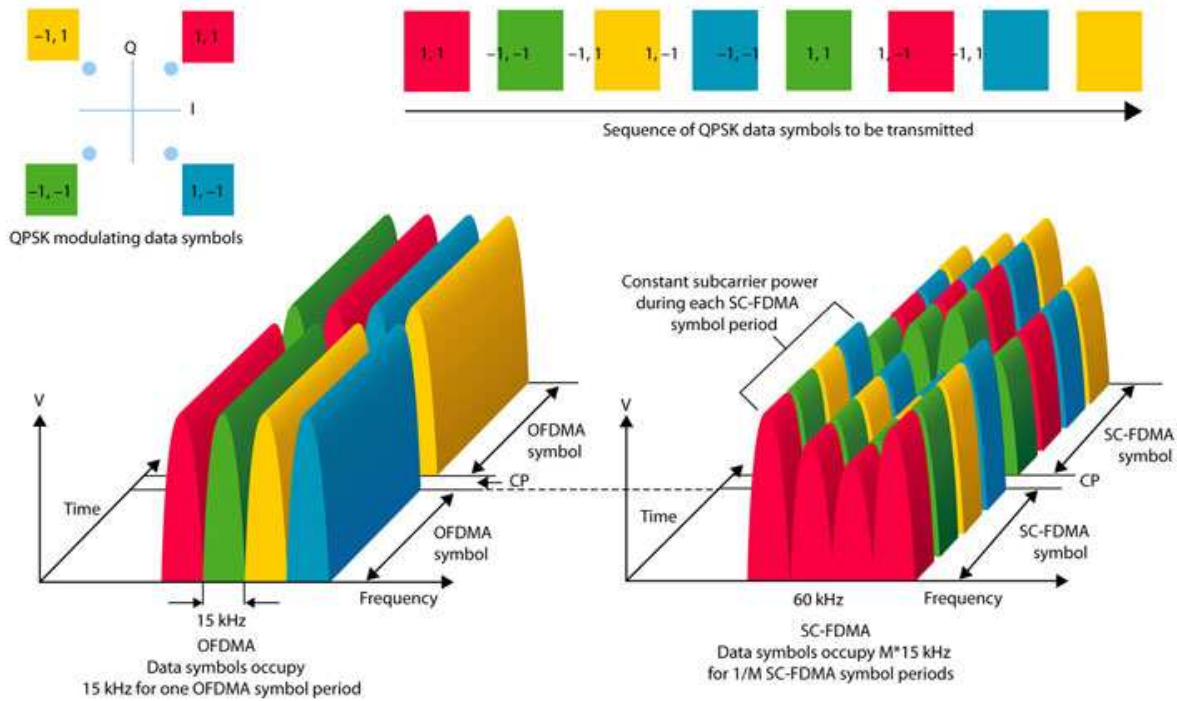
Figure 4: SC-FDMA in frequency domain [10]

2.3   Propagation and Fading

In communication, the quality of the received signal greatly depends on the propagation and fading during transmission. Here we can see some common types of fading and impairments of transmission channel.

2.3.1 Fading

RF signals propagate from antenna to different places through atmosphere. In atmosphere, signals can be affected by reflection, diffraction, scattering and absorption. At the receiver side, the signal arrives through several multipath and random fluctuations. These distortions in signal called fading which plays a vital role in communications. It can cause poor performance in a communication system which result in a loss of signal power without reducing the power of noise. There are different kind of fading models available for the distrivution of the attenuation. Here we can see major two models of fading [11]:

- Rician Fading: The Rician fading occurs when there is a LOS (line of sight) path available along with the number of indirect multipath signals.

- Rayleigh Fading: If there is no LOS path between transmitter and receiver and the transmission takes place only by multipath propagation; this type of fading called Rayleigh Fading. In this case, the received signal at the receiver is the sum of all the reflected and scattered waves.

2.3.2 Noise

Generally unwanted energy from different sources other than the transmitter is called Noise. Below are the some basic types of noise:

- Thermal Noise: Thermal noise is an excitation of the charge carriers inside the electric conductor and generated without applying any voltage source [12]. We can see it mathematically as:

N = KTW

Where,

T = Temperature in Kelvin

K = The Boltzmann Constant (K = 1.3806 x 10-23 Joules per Kelvin (J · K-1))

W = Bandwidth in Hz

N = Noise Power in Watts

- AWGN Noise: The AWGN (Additive white Gaussian noise) is a noise with continuous and uniform frequency spectrum over specified frequency band. It is often used as a channel model in which the only impairment to communicate is a linear addition of wideband or white noise with a constant spectral density and a Gaussian distribution of amplitude. The name denotes specific characteristics [13]:

    1. Additive: it is added to any noise that might be intrinsic to the information system.

    2. White: AWGN has uniform power across the frequency band for the information system similar to white color which has the uniform emissions at all frequencies.

    3. Gaussian: It consists of a normal distribution in the time domain with an average time domain value of zero.

- Cross talk: Cross talk appears due to inductive coupling between two closed wires or two adjacent subcarriers (inter-carrier interference). It is a very common scenario in telephone network where user experiences another user's voice in between the voice conversation.

- Intermodulation: When two different frequency signals are transmitted through a medium, then intermodulation occurs due to the nonlinear characteristic of the medium. It can come from co-channel interference, atmospheric conditions as well as man-made noise generated by medical, welding and heating equipment.

2.4   Attenuation

Attenuation is a general term that refers to any reduction in the strength of a signal over distances. A signal must be strong enough so that the receiver can detect and interpret the signal. If attenuation is too high then the receiver might not be able to identify the signal at all. [14] Attenuation is usually expressed in dB.

If P_s is the signal power at the transmitting end (source) of a communications circuit and P_d is the signal power at the receiving end (destination), then $P_s > P_d$. The power attenuation A_p in decibels is given by the formula:

$$A_p = 10 \log_{10}(P_s/P_d) \qquad \text{(i)}$$

2.5   Thesis Motivation

The Channel estimation is an imperative task to ensure efficient communication for 3GPP LTE network. It is essential before the demodulation of OFDM signals since the channel suffers from frequency selective fading and time varying factors for a particular communication system [9]. It is inevitable to evaluate the performance and stability of different kinds of channel estimation methods before activating at the practical field in order to promote a cost-efficient and smooth introduction and deployment.

The purpose of the thesis work is to evaluate the performance of LTE Downlink systems for various channel estimation algorithms under different channel conditions.

CHAPTER 3

OVERVIEW OF LTE PHYSICAL LAYER

LTE Physical layer translates data into reliable signal for transmission over a radio interface between eNobeB and the user equipment. It includes basic modulation, protection against transmission errors, multiplexing schemes as well as the antenna technology that are utilized. The antenna technology uses different configurations, schemes and techniques that can be incorporated into multiple antenna systems.

The LTE air interface consists of protocol layers where one of them is physical layer. Physical channels carry data from higher layers including control, scheduling and user payload (data) while the physical signals are used for system cell identification, radio channel estimation and system synchronization. The LTE air interface is designed for deployment in paired (FDD Mode) and unpaired (TDD mode) spectrum bands [15]. This thesis work is targeted or primarily based on LTE downlink transmission; therefore the bulk of the work is on the physical layer with focus on OFDMA and MIMO.

3.1   LTE Frame Structure

The LTE frame structure is comprised of two types,

- Type-1 LTE Frequency Division Duplex (FDD) mode systems
- Type-2 LTE Time Division Duplex (TDD) mode systems

Type-1 frame structure works on both half duplex and full duplex FDD modes. This type of radio frame has duration of 10ms and consists of 20 slots, each slot has equal duration of 0.5ms. Figure 5 shows a sub-frame consists of two slots, therefore one radio frame has 10 sub-frames. In FDD mode, downlink and uplink transmission is divided in frequency domain, such that half of the total sub-frames are used for downlink and half for uplink, in each radio frame interval of 10ms [16].
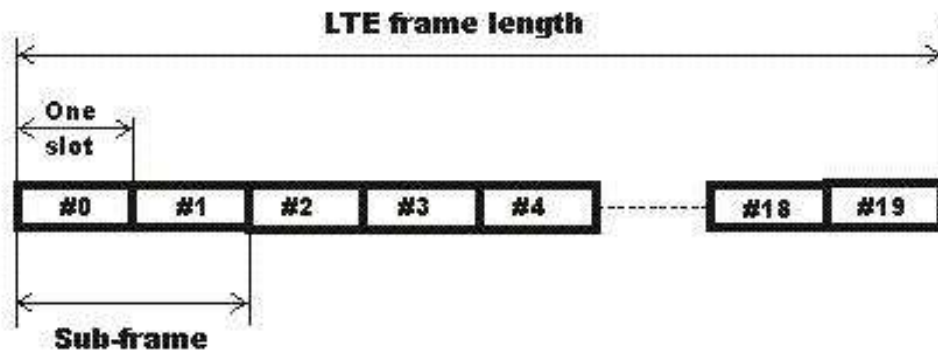
Figure 5: LTE Frame Length [8]

Type-2 frame structure is composed of two identical half frames of 5ms duration each. Both half frames have further 5 sub-frames of 1ms duration as illustrated in below figure 6:
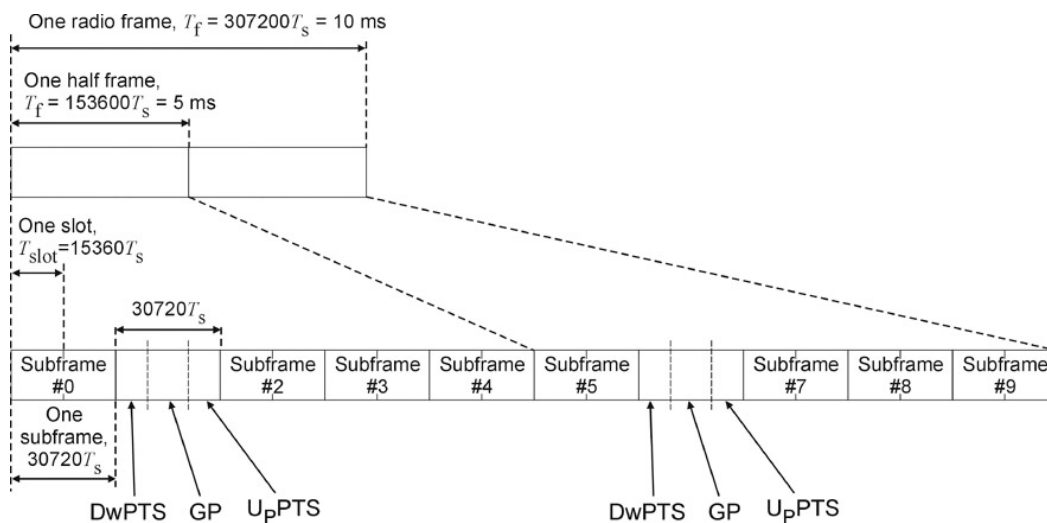
Figure 6: Type 2 Frame Structure [8]

13

One sub-frame consists of two slots and each slot has duration of 0.5ms. There are some special sub-frames which consist of three fields; Guard Period (GP), Downlink Pilot Timeslot (DwPTS) and Uplink Pilot Timeslot (UpPTS). In terms of length these three fields are configurable individually, but each sub-frames must have total length of 1ms [17].

Figure 7 shows the frequency representation of the LTE signal for OFDMA and SC-FDMA:
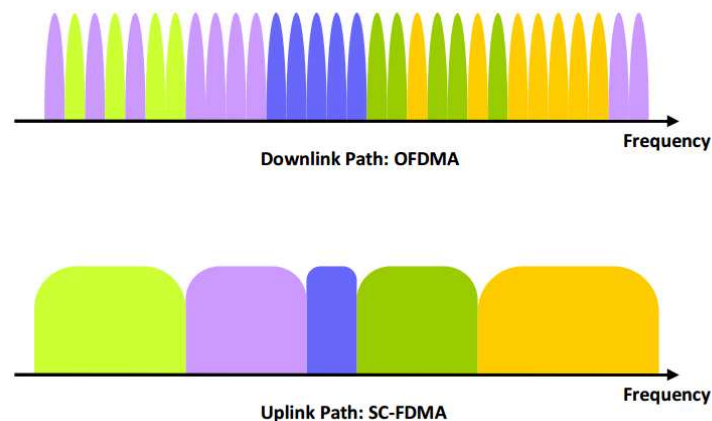
Figure 7: Frequency representation of OFDMA and SC-FDMA [18]

LTE Resource Block Architecture: The building block of LTE is a physical resource block (PRB) and all of the allocation of LTE physical resource blocks (PRBs) is handled by a scheduling function at the 3GPP base station (eNodeB). [19]

Figure 8 shows the below infirmatuion:

- 1 frame = 10 ms which consistes of 10 sub-frames

- 1 LTE subframe = 1 ms, which contains 2 slots

- 1 resource block = 0.5 ms which contains 12 subcarriers for each OFDM symbol in frequency domain

- 7 sysmbols (normal cyclic prefix) per time slot in the time domain or 6 sysm,bols in locg cyclic prefix
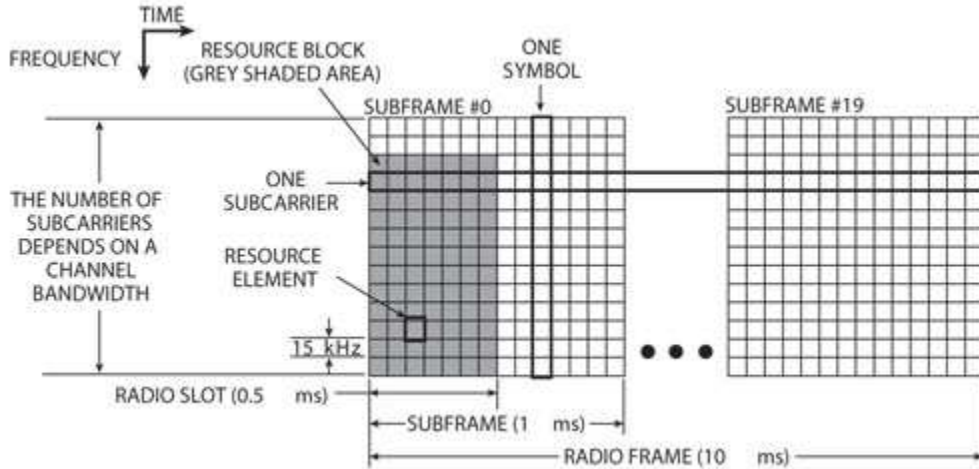
Figure 8: LTE resource block architecture [19]

3.2 Modulation Techniques

The modulation mapping methods available (for user data) are Quadrature Phase Shift Keying (QPSK), 16QAM and 64QAM. The use of QPSK modulation allows good transmitter power efficiency when operating at full transmission power. The devices will use lower maximum transmitter power when operating with 16QAM or 64QAM modulation. Figure 7 shows the number of bits/symbol for 3 different kinds of modulation mapping methods. For QPSK (Quadrature Phase Shift Keying) the bits/symbol is 2. Accordingly, the number of bits/symbol for 16 QAM (Quadrature Amplitude Modulation) and 64 QAM are 4 and 6.
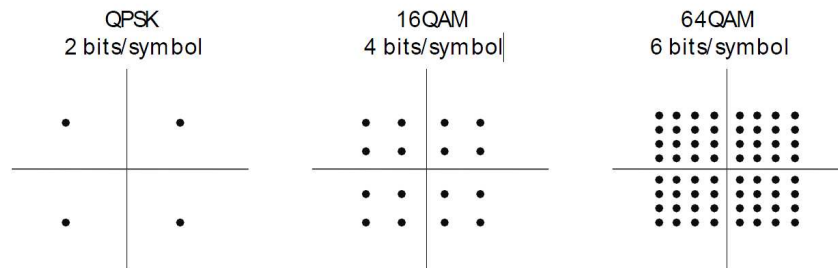
Figure 9: LTE Modulation Constellations [20]

3.3   Synchronization

A UE wishing to access an LTE cell must first undertake a cell search procedure. This consists of a series of synchronization stages by which the UE determines time and frequency parameters that are necessary to demodulate the downlink and to transmit uplink signals with the correct timing and the UE also acquires some critical system parameters. The synchronization signal is defined as the downlink physical signal which corresponds to a set of resource elements used by the physical layer but does not carry information originating from higher layers. The synchronization procedure makes use of two specially designed physical signals which are broadcast in each cell: the Primary Synchronization Signal (PSS) and the Secondary Synchronization Signal (SSS).The SSS carries the physical layer cell identity group and the PSS carries the physical layer identity. The detection of these two signals not only enables time and frequency synchronization, but also provides the UE with the physical layer identity of the cell and the cyclic prefix length, and informs the UE whether the cell uses Frequency Division Duplex (FDD) or Time Division Duplex (TDD) [21].

3.4   Frequency Allocations in LTE

There are different LTE band allocations for TDD and FDD. FDD requires pair bands and TDD requires a single band. Sometimes, these bands may overlap with each other. However, it is unlikely that both TDD and FDD transmissions could be present on a particular LTE frequency band [22].

Table 2 provides the chart of FDD frequency bands allocations along with the LTE band numbers and gaps. Accordingly, Table 3 provides the chart of TDD frequency bands allocations along with the LTE band numbers and width of bands.

FDD LTE BANDS & FREQUENCIES					
LTE BAND NUMBER	UPLINK (MHZ)	DOWNLINK (MHZ)	WIDTH OF BAND (MHZ)	DUPLEX SPACING (MHZ)	BAND GAP (MHZ)
1	1920 - 1980	2110 - 2170	60	190	130
2	1850 - 1910	1930 - 1990	60	80	20
3	1710 - 1785	1805 - 1880	75	95	20
4	1710 - 1755	2110 - 2155	45	400	355
5	824 - 849	869 - 894	25	45	20
6	830 - 840	875 - 885	10	35	25
7	2500 - 2570	2620 - 2690	70	120	50
8	880 - 915	925 - 960	35	45	10
9	1749.9 - 1784.9	1844.9 - 1879.9	35	95	60
10	1710 - 1770	2110 - 2170	60	400	340
11	1427.9 - 1452.9	1475.9 - 1500.9	20	48	28
12	698 - 716	728 - 746	18	30	12
13	777 - 787	746 - 756	10	-31	41
14	788 - 798	758 - 768	10	-30	40
15	1900 - 1920	2600 - 2620	20	700	680
16	2010 - 2025	2585 - 2600	15	575	560
17	704 - 716	734 - 746	12	30	18
18	815 - 830	860 - 875	15	45	30
19	830 - 845	875 - 890	15	45	30
20	832 - 862	791 - 821	30	-41	71
21	1447.9 - 1462.9	1495.5 - 1510.9	15	48	33
22	3410 - 3500	3510 - 3600	90	100	10
23	2000 - 2020	2180 - 2200	20	180	160
24	1625.5 - 1660.5	1525 - 1559	34	-101.5	135.5
25	1850 - 1915	1930 - 1995	65	80	15
26	814 - 849	859 - 894	30 / 40		10
27	807 - 824	852 - 869	17	45	28
28	703 - 748	758 - 803	45	55	10
29	n/a	717 - 728	11		
30	2305 - 2315	2350 - 2360	10	45	35
31	452.5 - 457.5	462.5 - 467.5	5	10	5

Table 2: FDD LTE frequency band allocations [20]

TDD LTE BANDS & FREQUENCIES		
LTE BAND NUMBER	ALLOCATION (MHZ)	WIDTH OF BAND (MHZ)
33	1900 - 1920	20
34	2010 - 2025	15
35	1850 - 1910	60
36	1930 - 1990	60
37	1910 - 1930	20
38	2570 - 2620	50
39	1880 - 1920	40
40	2300 - 2400	100
41	2496 - 2690	194
42	3400 - 3600	200
43	3600 - 3800	200
44	703 - 803	100

Table 3: TDD LTE frequency band allocations [7]

3.5   Downlink Parameters

As LTE has scalable bandwidth, the number of sub-carriers also changes while keeping sub-carriers spacing up to 15 khz. Additionally, there are two Cyclic Prefix are allowed (short and extended) [21] . Table 4 illustrates the LTE downlink parameters along with the transmission bandwidths, number of occupied sub-carriers and CP lengths.

Transmission BW		1.25 MHz	2.5 MHz	5 MHz	10 MHz	15 MHz	20MHz
Sub-carrier Duration T_{sub}		0.5ms					
Sub-carrier Spacing f_{space}		15kHz					
Sampling Frequency f_s		1.92 MHz	3.84MHz	7.68 MHz	15.36MHz	23.04 MHz	30.72 MHz
FFT and N_{IFFT}		128	256	512	1042	1536	2048
Number of occupied sub--carries N_{BW}		75	150	300	600	900	1200
Number of OFDM symbols per Sub-frame Short/Long (CP)		7/6					
CP Length $(\mu s / sample)$	short	(4.69/9)×6 (5.21/10)×1	(4.69/18)×6 (5.21/20)×1	(4.69/18)×6 (5.21/40)×1	(4.69/72)×6 (5.21/80)×1	(4.69/108)×6 (5.21/120)×1	(4.69/144)×6 (5.21/160)×1
	Long	(16.67/32)	(16.67/64)	(16.67/128)	(16.67/256)	(16.67/384)	(16.67/512)

Table 4: LTE Downlink parameters [18]

3.6   Multiple Antenna Techniques

MIMO antenna technology is one of the key technologies leveraged on by LTE. It is a technology in which multiple antennas are used at both the transmitter and at the receiver for enhanced communication: The use of additional antenna elements at either the base station (eNodeB) or User Equipment side (on the uplink and/or downlink) opens an extra spatial dimension to signal precoding and detection [22]. Depending on the availability of these antennas at the transmitter and/or receiver, the following classifications exist:

- Single-Input Multiple-Output (SIMO): A simple scenario of this is an uplink transmission whereby a multi-antenna base station (eNodeB) communicates with a single antenna User Equipment (UE).

- Multiple-Input Single-Output (MISO): A downlink transmission whereby a multi-antenna base station communicates with a single antenna User Equipment (UE) is a scenario.

- Single-User MIMO (SU-MIMO): This is a point-to-point multiple antenna link between a base station and one UE.

- Multi-User MIMO (MU-MIMO): This features several UE□s communicating simultaneously with a common base station using the same frequency- and time-domain resources.

As a result of the requirements on coverage, capacity and data rates, integration of MIMO as part of the LTE physical layer is highly imperative since it necessitates the incorporation of transmission schemes like transmit diversity, spatial multiplexing and beam forming.

CHAPTER 4

LITERATURE REVIEW

4.1   Introduction to Channel Estimation in OFDMA

In this chapter, different kinds of channel estimation techniques are described for LTE downlink systems. The effect of the channel on the transmitted information must be estimated in order to recover the transmitted information signal correctly. There are various kinds of radio propagation channel which are mainly effective for different channel estimation algorithms [4]. If the receiver can keep the track of the varying radio propagation channels, it can efficiently recover the transmitted information.

4.2   OFDM Signal Model

We consider an OFDM symbol to perform channel estimation in LTE downlink system. Below is the equation of our signal model, where we consider a diagonal matrix containing the transmitted frequency domain samples and the channel frequency response vector [23]:

$$Y = XH + \mu \quad \text{(ii)}$$

$X \ \square \ C^{N}{}_{\text{IFFT}}{}^{X \ N}{}_{\text{IFFT}}$ is a diagonal matrix

$H \ \square \ C^{N}{}_{\text{IFFT}}$ contains unknown channel frequency response coefficients

$\mu \ \square \ C^{N}{}_{\text{IFFT}}$ is the noise vector.

We can write the channel frequency response (CFR) in terms of channel impulse response (CIR) as,

$$H = Fh \qquad \text{(iii)}$$

So we will get then:

$$Y = XFh + \mu \qquad \text{(iv)}$$

Where,

Y = Channel Impulse Response

$F \square C^{\text{NIFFT x NIFFT}}$ is DFT matrix

4.3 Pilot-assisted Channel estimation

There are different kinds of pilot-assisted channel estimation schemes that can be deployed for the estimation of the channel effects on the transmitted signal. Interpolation methods determine the response of the channel at the data subcarriers. We used several interpolation methods to get the simulation results for channel estimations such as: Linear, Piecewise constant, Averaged and Pilot averaged [24].

4.3.1 Least Square Estimation (LSE)

In this channel estimation technique, the channel impulse response is determined from the known transmitted reference symbols according to the following equations [25]:

$$G_{LS} = \left[\frac{Yr(1)}{Xr(1)}, \frac{Yr(2)}{Xr(2)}, \frac{Yr(3)}{Xr(3)}, \frac{Yr(4)}{Xr(4)} \cdots \frac{Yr(N)}{Xr(N)} \right] \qquad \text{(v)}$$

Here,

$G_{LS} \square C^{Nr}$ is the estimated channel frequency response on the subcarriers.

Xr and Yr are the corresponding number of the received signal.

In order to obtain the channel frequency response for the subcarriers carrying data symbols, this

response can be interpolated over full frequency range whether it could be in time domain or frequency domain.

The time domain signal can be expressed as:

$$Y_r = F_H A_r F_L h + \mu \qquad \text{(vi)}$$

Where,

h is the L x 1 vector corresponding to the FIR representation of the channel in the time domain.

F_L is the N x L Fourier matrix that gives the frequency domain representation over N sub-carriers of the channel of length.

A is the N x N diagonal matrix containing, in the positions corresoponding to the modulated sub-carriers (N_m over N), the transmitted symbols (comprising both data and pilot) in the frequency domain, assumed to be transmitted with the same energy.

F_H is the N x N inverse Fourier matrix giving the time domain representation of the received signal.

μ is the N x 1 vector corresponding to the complex circular additive white Gaussian noise.

So, the channel estimation using Least Squares in time domain can be expressed in the following way:

$$\hat{h} = (S^H S)^{-1} S^H Y_r \qquad \text{(vii)}$$

Where,

The matrix S is an approximation where the pilot symbols are taken into account

Finally, we can get the expression for LS estimate by solving above equations:

$$\hat{h} = (F_L^H A_r^H A_r F_L)^{-1} F_L^H A_r^H F^H Y_r \qquad \text{(viii)}$$

Where,

$(F_L^H A_r^H A_r F_L)^{-1} F_L^H$ is constant and we can solve it regardless of the time varying nature of the channel.

4.3.2 Minimum Mean Square Estimation (MMSE)

The Least Square estimation technique is computationally simple but the performance is not that efficient. The Channel Impulse Response for Minimum Mean Square Estimator (MMSE) has better performance even though it is computationally complex. Here is the equation for CIR of Linear Minimum Mean Square Estimator [25]:

$$\hat{h} = R_{hYr} R_{YrYr}^{-1} Y_r \qquad \text{(ix)}$$

Where,

$\hat{h}$ channel is considered as a deterministic parameter

R_{YrYr} is the auto covariance of vector Yr.

R_{hYr} is the cross covariance of vectors h and Yr.

The values for R_{hYr} and R_{YrYr} are given below:

$$R_{YrYr} = X_r T_r R_{hh} X_r^H T_r^H + \sigma_\mu^2 IN_r \qquad \text{(x)}$$

$$R_{hYr} = X_r^H T_r^H \qquad \text{(xi)}$$

So, finally we got the equation:

$$\hat{H} = X_r^H T_r^H (X_r T_r R_{hh} X_r^H T_r^H + \sigma_\mu^2 IN_r)^{-1} Y_r \qquad \text{(xii)}$$

Where,

R_{YrYr} is the auto covariance of vector Yr

R_{hYr} is the cross covariance of vectors h and Yr

σ_μ is the constant parameter

T_r^H is the channel co-factor

CHAPTER 5

SIMULATIONS AND RESULTS

5.1   Software Overview - LTE PHY Lab

I have used the LTE PHY LAB Software for our simulation and experimental results [2]. It has a form of MATLAB toolbox which is very user friendly and convenient for modeling and simulating the communication systems. I used the version 1.2 for my simulation, which is a comprehensive implementation of the 3GPP Release 8 E-UTRA physical layer [26].

5.1.1 LTE PHY LAB v.1.2 Features

These are the main features for using the software [27, 28]:

- Downlink and uplink (including RACH) support

- FDD support (TDD available on request)

- Normal and Extended CP

- Support for MIMO (SM (SU-MIMO), TX diversity),

- OFDMA and SC-FDMA

- MIB generation and decoding

- DCI generation and blind decoding

- Feedback generation and decoding (CQI, PMI, RI estimation)

- Flexible control of all the necessary parameters, e.g.:

- Resource allocation (number and placement of resource blocks)

- Input bits for data and control channels

- MIMO configuration (number of antennas and mode of operation)

- MCS (modulation, transport block size, redundancy version)

- System parameters (UE and Cell IDs, system BW, control area size, UL channels' configuration)

- Support for all the LTE bandwidths: 1.4MHz, 3MHz, 5MHz, 10MHz, 15MHz, 20MHz

- Channel models included (AWGN, SUI, E-UTRA 3GPP TS 36.101)

- Test files included (see user guide for example usages)

- Use case scenarios (e.g. UL feedback generation, system sync procedure)

- Possibility to combine with other MATLAB functions and Toolboxes (e.g. Signal Processing Toolbox and Communications Toolbox)

- Implemented supporting transmitter algorithms

  - PAPR Reduction for downlink and uplink

- Implemented supporting receiver algorithms

  - Channel estimation and correction for downlink and uplink

  - Time and frequency synchronization for downlink and uplink

5.1.2 LTE PHY LAB v.1.2 Downlink Channels and Signals

In table 5, we can see the information of the transport and physical channels for downlink. Accordingly, in figure 10, the transport and PHY channel baseband processing within eNB transmitter.

	Transport channels and control information	Physical channels and signals
Downlink	DL-SCH, BCH, CFI, HI, DCI	PDSCH, PBCH, PDCCH, PCFICH, RS, P-SS, S-SS

Table 5: Downlink Channels and Signals [2]
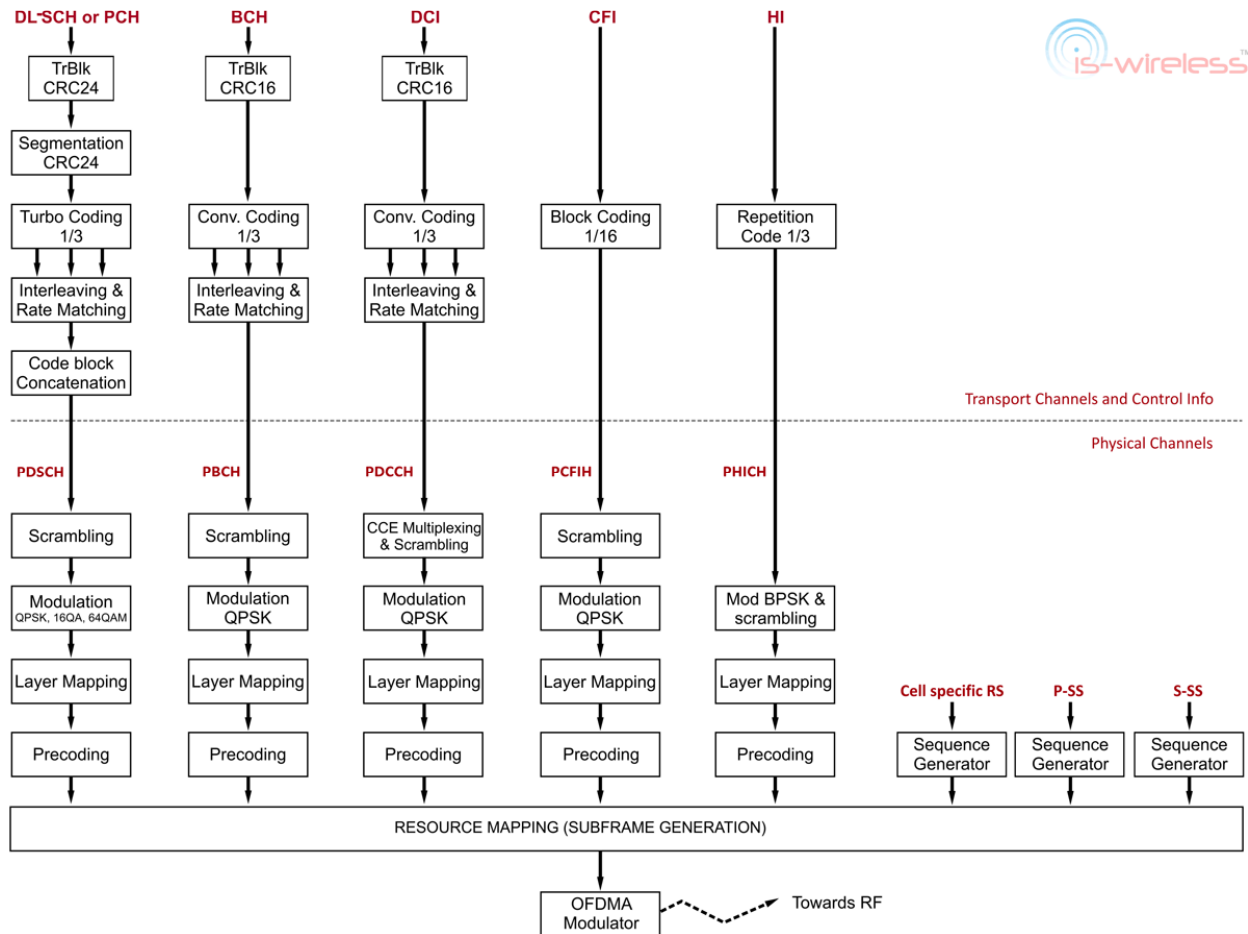
Figure 10: Transport and PHY channel baseband processing within eNB transmitter [2]

5.2   Simulation Results and Analysis

The Figure 11 shows the subfunctions of downlink processing chain including the supporting algorithms in PHY layer [2]. When the transport channels are processed through the MAC layer, it starts the baseband processing with PHY layer and generates PHY channels and input output signals. Afterwards, in the part of resource mapping, the subframes are generated to modulate in the OFDMA modulator. PAPR reduction would be processed before the OFDMA modulator process the data. Channel estimation has been done at the UE PHY receiver side.
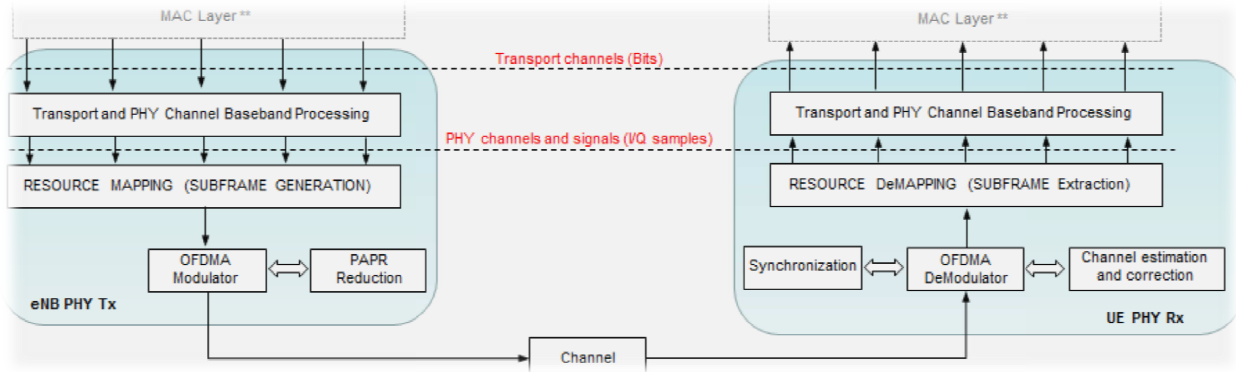
Figure 11: LTE PHY Lab Downlink processing Chain Flow Chart [2]

The Software LTE PHY LAB followed the standard of 3GPP specifications standard. The relation between implementation of the LTE PHU LAB and the 3GPP specifications is shown in figure 12. Each function of this software implements the 3GPP LTE specifications. The user can build its own system based on that functions. Additionally there are functions (called gathering functions) building up the whole processing chains of transmitters and receivers. [2]
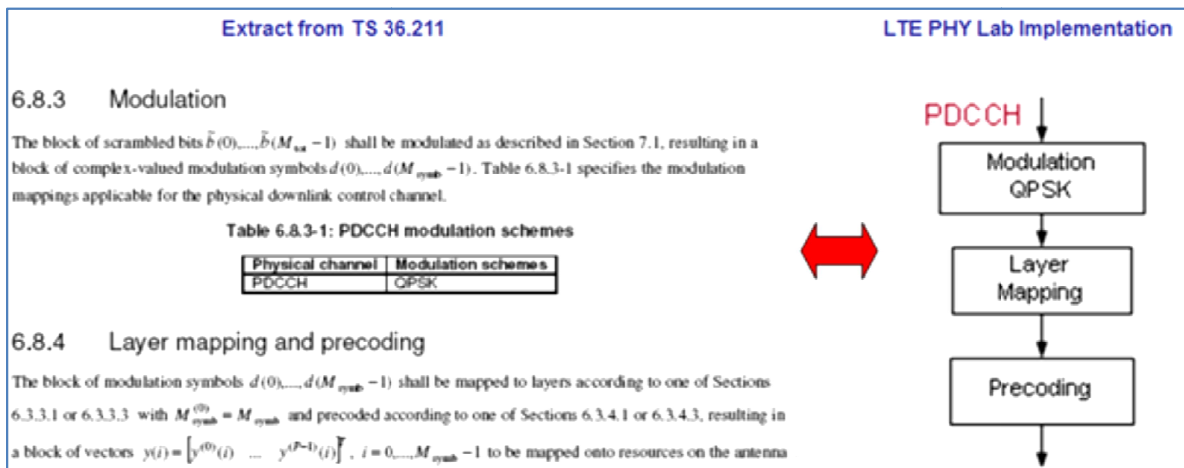
Figure 12: Relation between 3GPP specification and LTE PHY LAB implementation [2]

In the table 6 below, we can see a flow diagram of parameters I have used for simulation part at transmitter side.

```
┌─────────────────────┐     ┌─────────────────────┐     ┌─────────────────────┐
│ LTE Link Level      │     │ LTE DL Phy          │     │ OFDM Modulation -   │
│ Simulate DL         │ ──▶ │ Transmitter -       │ ──▶ │ Generates one OFDM  │
│ - Simulates 1 DL    │     │ Performs processing │     │ symbol              │
│ radio frame         │     │ and transmission    │     │                     │
│ (Transmission over  │     │ of one subframe     │     │                     │
│ multipath channel)  │     │                     │     │                     │
└─────────────────────┘     └─────────────────────┘     └─────────────────────┘
                                                                   │
                                                                   ▼
┌─────────────────────┐     ┌─────────────────────┐     ┌─────────────────────┐
│ Layer Mapping -     │     │ MIMO Precoding -    │     │ DL Resource Mapping │
│ Performs layer      │ ◀── │ Performs precoding  │ ◀── │ - Maps all physical │
│ mapping for all     │     │ for all             │     │ channels on the TF  │
│ schemes (SISO, Tx   │     │ multiantenna        │     │ grid for one        │
│ Diversity, SM)      │     │ schemes             │     │ subframe            │
└─────────────────────┘     └─────────────────────┘     └─────────────────────┘
```

Table 6: Simulation flow diagram for Transmitter [2]

In table 7, we can see a flow diagram of parameters I have used for simulation part at receiver side.
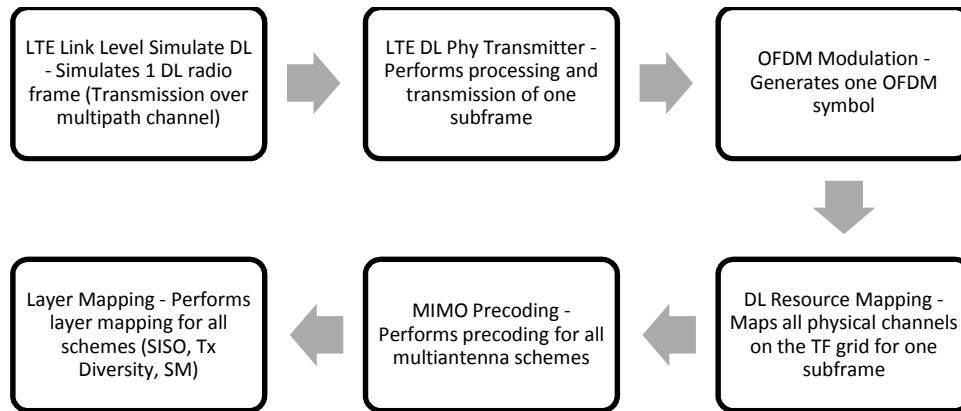
```
┌─────────────────────┐     ┌─────────────────────┐     ┌─────────────────────┐
│ LTE DL Phy          │     │ OFDM DeModulation - │     │ DL Resource         │
│ Receiver -          │     │ Demodulates one     │     │ DeMapping - Demaps  │
│ Performs processing │ ──▶ │ OFDM symbol         │ ──▶ │ all physical        │
│ and reception of    │     │                     │     │ channels from the   │
│ one DL subframe     │     │                     │     │ TF grid for one     │
│                     │     │                     │     │ subframe – as a     │
│                     │     │                     │     │ generates vector of │
│                     │     │                     │     │ samples for each    │
│                     │     │                     │     │ physical channel    │
└─────────────────────┘     └─────────────────────┘     └─────────────────────┘
                                                                   │
                                                                   ▼
┌─────────────────────┐     ┌─────────────────────┐     ┌─────────────────────┐
│ DL Noise Estimation │     │ Layer DeMapping -   │     │ MIMO DePrecoding -  │
│ - Performs noise    │ ◀── │ Performs layer      │ ◀── │ Performs decoding   │
│ estimation in       │     │ demapping for       │     │ for multiantenna    │
│ downlink            │     │ multiantenna        │     │ schemes (SISO,      │
│                     │     │ schemes (SISO, Tx   │     │ Tx/Rx Diversity,    │
│                     │     │ Diversity, SM)      │     │ SM)                 │
└─────────────────────┘     └─────────────────────┘     └─────────────────────┘
       │
       ▼
┌─────────────────────┐
│ DL Resource         │
│ DeMapping Select -  │
│ Performs selected   │
│ resource demapping  │
│ for the downlink    │
│ subframe.           │
└─────────────────────┘
```
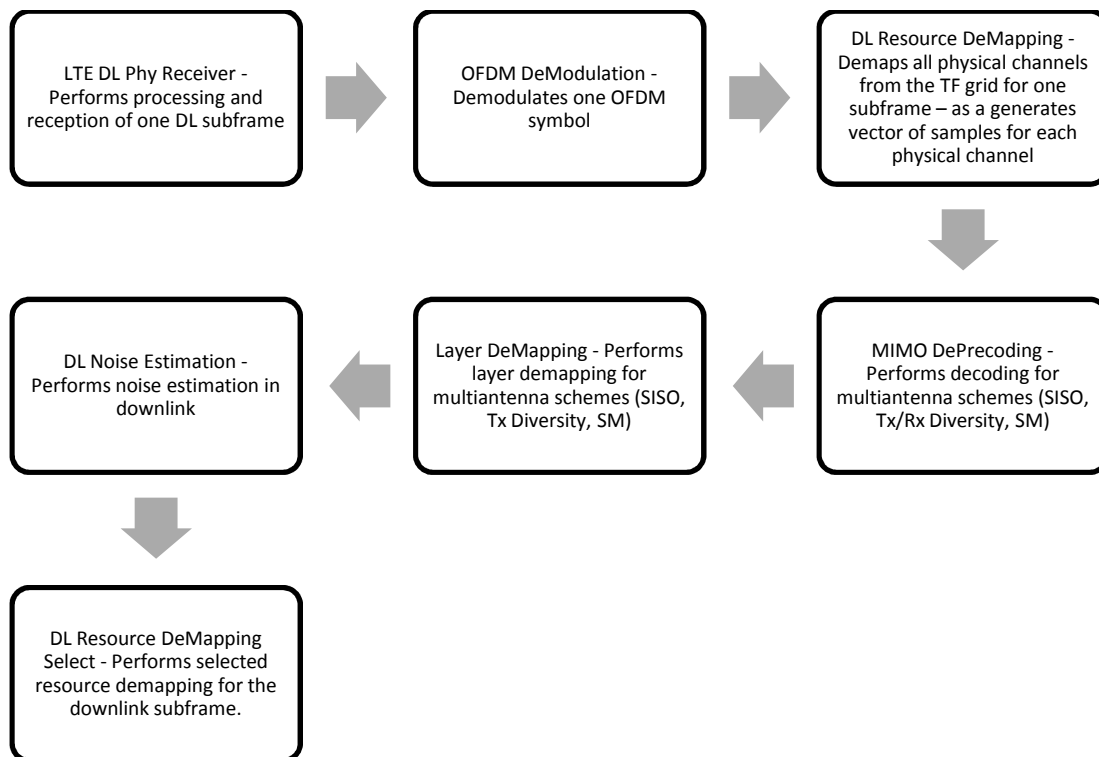
Table 7: Simulation flow diagram for Receiver [2]

In table 8, we can see a flow diagram of parameters I have used for simulation part at channel estimation.
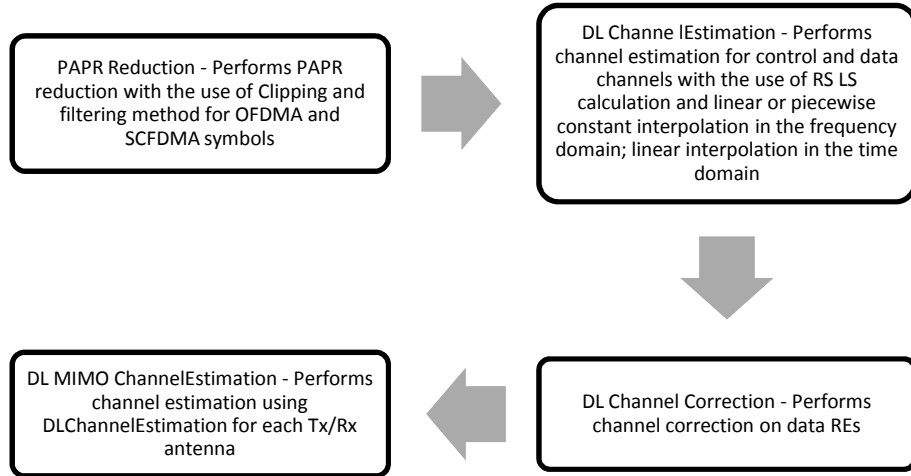


```
┌─────────────────────────┐         ┌─────────────────────────────┐
│  PAPR Reduction - Performs PAPR  │    →    │  DL Channe lEstimation - Performs  │
│  reduction with the use of Clipping and │         │  channel estimation for control and data  │
│  filtering method for OFDMA and │         │  channels with the use of RS LS  │
│  SCFDMA symbols │         │  calculation and linear or piecewise  │
│                         │         │  constant interpolation in the frequency  │
│                         │         │  domain; linear interpolation in the time  │
│                         │         │  domain  │
└─────────────────────────┘         └─────────────────────────────┘
```

```
┌─────────────────────────────┐         ┌─────────────────────────────┐
│  DL MIMO ChannelEstimation - Performs  │    ←    │  DL Channel Correction - Performs  │
│  channel estimation using │         │  channel correction on data REs  │
│  DLChannelEstimation for each Tx/Rx │         │  │
│  antenna │         │  │
└─────────────────────────────┘         └─────────────────────────────┘
```

Table 8: Simulation flow diagram for Channel Estimation [2]

5.2.1 Frame level simulation of Downlink and Uplink

After generating PHY layer samples of the 3GPP E-UTRA Rel 8 downlink radio frame type 1, normal and extended CP, we have simulated downlink transmission and reception of a LTE FDD system under various parameters. Here is the value of the parameters we set for initial simulation in LTE PHY LAB:

Input matrix of the HI (of size (number of subframes) X (number of HIs)), txHI = randint(10, 8, 2)

For FFTsizes: 128 – 512 : 8 HIs

1024, 1536 : 16 HIs

And 2048 : 24 HIs

sizeFFT = number corresponding to the fft size (related to the system BW), (values: 128, 256, 512, 1024, 1536, 2048), sizeFFT = 128

SNR = randint(1,10,10)*10 + 30

Physical cell ID (0 - 503), N_cell_ID = 13

radio frame number, nF = 0

CPtype = 1

In figure 13, we can see the simulated result for the above parameters. The horizontal axis refers to the times for 10 sub frames and the vertical axis refers to the magnitude. This reference signal is being transmitted at every subframe and it spans all across the operating bandwidth. In this case, we have set the parameter of FFT is 128.
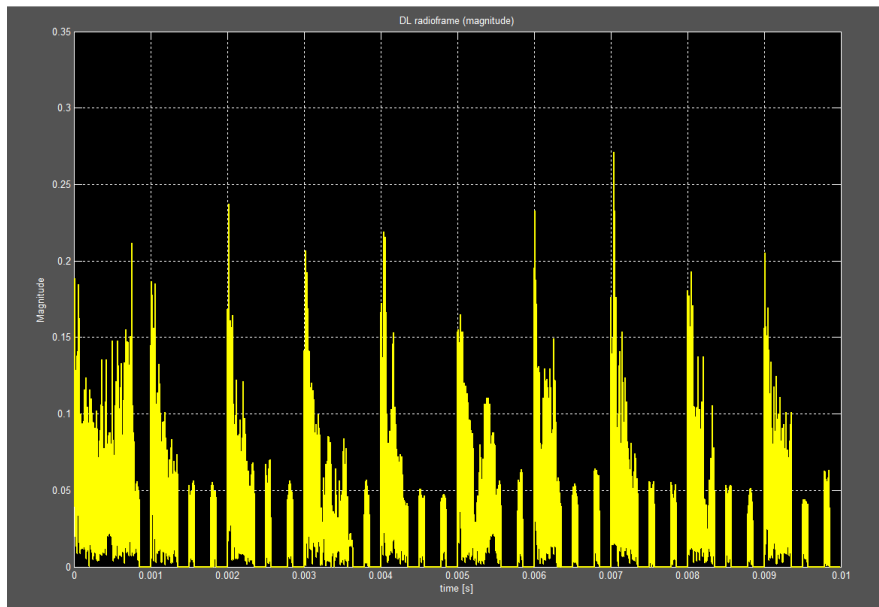

Figure 13: Time domain signal magnitude of a LTE DL radio frame

5.2.2 Generating AWGN noisy output channel

In this case, we transmit the input samples over the AWGN channel and generated the noisy output samples. We set the below parameters in LTE PHY LAB:

SNR = signal to noise ratio given in dB = 30

We set two random variables first to get AWGN noisy samples: (Table 9)

```
a =

    1   0   1   0   1   1   1   0   1   0   1   0   1   1   1   0   0   1   1   1
>> b

b =

    1   0   1   0   1   1   0   1   0   1   0   0   0   0   1   0   0   0   0   0
```

Table 9: Two Random Variables

And here are the Rx output samples:

According to the Rx data what we got from the simulation, we can see that for SNR 30, the time domain OFDM symbols become noisy as yellow marked data in the matrix output. (Table 10)

```
RxData =

  Columns 1 through 7

    1.0135 + 0.9738i   0.0009 + 0.0056i   0.9769 + 0.9941i   -0.0291 - 0.0182i   0.9705 + 1.0030i   0.9938 + 0.9735i   0.9548 + 0.0076i

  Columns 8 through 14

    0.0091 + 0.9644i   0.9980 - 0.0549i   -0.0077 + 0.9953i   1.0146 - 0.0220i   0.0077 + 0.0342i   0.9923 + 0.0307i   1.0007 - 0.0137i

  Columns 15 through 20

    0.9970 + 0.9784i   -0.0140 - 0.0048i   0.0249 - 0.0071i   1.0269 + 0.0310i   1.0016 - 0.0078i   0.9770 + 0.0270i
```

Table 10: Time Domain OFDM matrix symbol with AWGN noise

5.2.3 Error Vector Magnitude (EVM) Calculation

EVM measurement requires apriori knowledge of transmitted symbol, or must assume that closest constellation point is transmitted symbol. EVM is normalized to average power. EVM may be easily computed from a modulated signal because:

- SNRs are extremely high so that the measured EVM represents transmitter constellation distortion, and not noise-induced signal distortion.
- High SNRs for measurement means that nearest constellation point is always the transmitted constellation point, I.e BER = 0 for transmitter testing purposes [29]

These are parameters we set sample values for transmitter and receiver symbols to get the simulated results of EVM.

txSymbols = matrix of samples of the transmitted subframes = complex(randint(14,128,2), randint(14,128,2))

rxSymbols = matrix of samples of the receive subframes = complex(randint(14,128,2), randint(14,128,2))

We got the below EVM simulated result for below parameters (Only column 1 through 26 of 128 have been shown here). In this case, we can see that the simulated matrix data of EVM has been distorted which represent the transmitter constellation distortion. A single point is ideal, but in practice there will be a cluster of actual points around the ideal point. The more widespread the points, the poorer the EVM. (Table 11)

```
EVM =

Columns 1 through 13

    1.4142        0   1.4142   1.4142        0   1.0000   1.0000   1.0000   1.0000   1.0000   1.0000   1.0000   1.0000
         0   1.0000        0   1.4142   1.0000   1.0000   1.4142   1.0000   1.0000   1.4142   1.0000   1.0000   1.0000
    1.0000   1.0000   1.0000   1.4142   1.4142        0        0   1.0000        0   1.4142   1.0000   1.0000        0
    1.0000   1.0000   1.0000        0   1.0000        0        0   1.0000   1.0000        0   1.0000        0   1.0000
         0   1.4142   1.4142   1.4142        0   1.0000   1.4142   1.0000        0        0   1.4142   1.0000   1.0000
    1.0000   1.0000   1.4142   1.0000   1.0000   1.0000   1.0000   1.0000        0        0   1.0000        0   1.4142
    1.4142   1.4142        0        0   1.0000        0   1.4142   1.0000   1.0000        0   1.0000   1.4142   1.4142
    1.0000   1.4142   1.0000   1.4142   1.0000   1.0000   1.0000        0   1.4142   1.0000   1.0000        0   1.0000
         0        0   1.4142   1.0000   1.0000   1.0000   1.4142        0   1.0000        0        0   1.4142   1.0000
    1.4142   1.4142        0        0   1.4142   1.4142   1.0000   1.0000        0   1.4142   1.0000   1.0000   1.0000
    1.4142   1.0000   1.4142        0   1.4142        0   1.0000   1.0000        0   1.0000   1.0000   1.0000   1.4142
    1.0000   1.0000   1.0000   1.4142   1.0000        0   1.0000   1.4142   1.0000   1.0000   1.0000   1.4142        0
         0   1.0000        0   1.0000   1.4142   1.0000   1.0000   1.4142        0   1.4142   1.4142        0   1.0000
         0   1.0000   1.0000        0   1.0000   1.0000   1.4142   1.0000   1.0000   1.0000   1.0000   1.0000   1.0000

Columns 14 through 26

         0   1.0000        0   1.4142   1.0000   1.0000   1.4142   1.4142   1.0000   1.0000        0   1.0000   1.0000
    1.4142   1.4142   1.0000   1.4142   1.0000   1.0000        0   1.0000        0   1.0000   1.4142   1.0000   1.0000
    1.0000   1.0000   1.4142        0        0   1.4142   1.0000   1.0000   1.0000   1.4142   1.0000   1.0000        0
    1.0000   1.4142   1.4142   1.4142   1.0000   1.4142   1.0000        0   1.0000   1.0000   1.0000   1.0000   1.0000
         0   1.4142   1.4142   1.0000   1.0000        0   1.0000        0   1.0000   1.0000        0        0        0
         0   1.0000   1.0000        0   1.4142        0        0   1.0000        0   1.0000   1.0000   1.0000   1.0000
    1.0000   1.4142   1.0000        0   1.4142   1.4142   1.4142   1.0000   1.4142        0   1.0000   1.0000   1.0000
    1.0000   1.4142   1.4142   1.4142   1.0000   1.0000   1.0000   1.4142   1.4142        0        0   1.0000   1.4142
    1.4142        0        0   1.0000   1.4142        0        0   1.0000   1.0000        0   1.0000        0        0
    1.0000   1.0000        0   1.0000        0   1.0000   1.0000   1.0000   1.0000   1.0000   1.0000   1.0000   1.0000
         0   1.0000   1.4142   1.4142   1.0000        0   1.0000   1.0000        0   1.4142   1.4142        0   1.0000
         0   1.4142   1.0000   1.4142   1.0000        0        0   1.0000        0   1.4142        0   1.0000        0
         0   1.0000   1.4142   1.0000   1.0000   1.4142   1.0000   1.0000        0        0   1.0000   1.4142   1.0000
    1.0000   1.0000   1.0000   1.4142   1.4142   1.4142   1.4142   1.0000   1.0000   1.0000   1.4142   1.0000   1.4142
```

Table 11: EVM Matrix Data

5.2.4 Sub frame Synchronization

In LTE, there are two downlink synchronization signals which are used by the UE to obtain the cell identity and frame timing [30].

- Primary synchronization signal (PSS)
- Secondary synchronization signal (SSS)

In this case, we performed subframe synchronization algorithm. It determines the time offset for whole subframe, correlating the received subframe with locally generated PSS signals (three types), SSS signal and determine N_cell_ID.

Here are the values of the parameters we set for sub frame synchronization of downlink:

txHI = randint(1,16,2)

modOrder = 64

numSubframe = 0

sizeFFT = 1024

numPDCCH = 3

numsPRB = [2 3 4 5]

N_cell_ID = 124

PHICHtype = 0

CPtype = 0

5.2.5 Downlink frequency synchronization

According to [30], for frequency synchronization for OFDMA system is required coarse and fine frequency synchronization. Coarse frequency synchronization estimates integer frequency offset and fine frequency synchronization estimates fraction frequency offset. In general, PSS correlation based estimation method and CP correlation based tracking loop are applied for coarse and fine frequency synchronization in 3GPP LTE OFDMA system,

respectively [31]. However, the conventional coarse frequency synchronization method has performance degradation caused by fading channel and SNR loss. Also, the conventional fine frequency synchronization method cannot guarantee stable operation in TDD mode because there is no signal in uplink subframe.

In this case, we set the below values for desired parameters in LTE PHY LAB:

FFTsize = FFT size used in transmitter: 128 (default), 256, 512, 1024, 1536 or 2048 =128;

numOFDMSym = 14

TimeOffsetFractional = 0

numSubframe = subframe number (0 - 9) = 0

numAntennas = [1 1]

idxAntenna = number of mapping antena (with PSS signal) = 1

CPtype = measured CP type (0 - normal, 1 extended) = 0

N_ID_2 = index of received PSS signal 0, 1 or 2 for each type =1

After the simulation done, I got the below results for receiver resource grid (Only columns 1 through 44 of 128 has been shown here). As I used the coarse frequency synchronization for the simulation, it estimates integer frequency offset. However, the red indicated matrix data signifies the performance degradation caused by fading channel and SNR loss. (Table 12)

Table 12: Receiver resource grid in matrix form

5.2.6 Downlink Noise Estimation

To measure the noise estimation in downlink, we performed several algorithm steps, which are [32]:

- Averaging pilots
- Channel estimation
- Noise estimation

We set some sample values for specific parameters in LTE PHY LAB to get the noise estimation in downlink.

FFTsize = size of the FFT used in OFDMA modulation = 128;

numOFDMSym = 14;

CPtype = measured CP type = 0;

N_cell_ID = Physical layer cell ID (0 - 503) = 2;

numSubframe = subframe number (0 - 9) = 0;

numAntennas = number of antennas used for transmission [Tx, Rx] = [1 1];

nF = radio frame number = 0;

After simulation done, we got the below results:

Average Noise Power = 0.40

Average Noise SNIR = 0.76

5.2.7 Peak to Average Power Ratio (PAPR) Reduction

Peak to Average Power Ratio (PAPR) reduces the efficiency of the transmit high power amplifier. Due to the large number of sub-carriers in typical OFDM systems, the amplitude of the transmitted signal has a large dynamic range, leading to in-band distortion and out-of-band radiation when the signal is passed through the nonlinear region of power amplifier [33, 34]. Although the above-mentioned problem can be avoided by operating the amplifier in its linear region, this inevitably results in reduced power efficiency.

 We performed Peak to Average Power Ratio reduction in the following steps:

 - CP removing

 - Truncation threshold calculation for specified clipping factor

 - Oversampling (not implemented yet)

 - OFDMA/SCFDMA symbols truncation using threshold determined in previous step

 - Filtering (to remove DC and OOB distortions)

 - Down sampling

 - CP adding

We set the below parameters some sample values in LTE PHY LAB:

inputSymbols = input complex NxM matrix of OFDMA/SCFDMA symbols (time domain). Each must be in separate row of input matrix. N = 1,2,.. MAX = complex(a,b)

FFTsize = size of the FFT block: 128, 256, 512, 1024, 1536, 2048 = 128

CPver = cyclic prefix version: 0 (first symbol in slot), 1 (second symbol in slot). It must have the same number of rows as inputSymbols = 1

CPtype = 0

After setting the above parameters, we got the below results (table 13) for PAPR reduction in matrix form. According to the simulated result, the PAPR reduction samples are denoted by yellow marks. High PAPR in the matrix data is observed due to large dynamic range of its symbol waveforms. As we know that this high PAPR forces the High Power Amplifier (HPA) to have a large back-off in order to ensure linear amplification of the signal, which significantly reduces the efficiency of the amplifier.

```
Columns 1 through 7

  0.0386 + 0.0030i  -0.0305 + 0.0559i  -0.0232 + 0.0777i   0.0295 + 0.0289i   0.0300 - 0.0224i  -0.0033 - 0.0273i  -0.0079 - 0.0317i

Columns 8 through 14

 -0.0029 - 0.0398i  -0.0088 + 0.0111i   0.0063 + 0.0831i   0.0285 + 0.0633i   0.0070 - 0.0195i  -0.0325 - 0.0392i  -0.0304 - 0.0085i

Columns 15 through 21

 -0.0056 - 0.0277i   0.0022 - 0.0616i   0.0131 - 0.0133i   0.0269 + 0.0649i  -0.0070 + 0.0635i  -0.0644 + 0.0198i  -0.0492 + 0.0334i

Columns 22 through 28

  0.0219 + 0.0822i   0.0288 + 0.0782i  -0.0338 + 0.0229i  -0.0484 - 0.0125i   0.0118 - 0.0074i   0.0521 - 0.0097i   0.0287 - 0.0413i

Columns 29 through 35

  0.0005 - 0.0584i   0.0171 - 0.0370i   0.0516 - 0.0245i   0.0508 - 0.0449i   0.0133 - 0.0430i  -0.0037 + 0.0026i   0.0298 + 0.0212i

Columns 36 through 42

  0.0636 - 0.0171i   0.0470 - 0.0332i   0.0164 + 0.0102i   0.0300 + 0.0314i   0.0649 - 0.0130i   0.0613 - 0.0446i   0.0225 - 0.0159i

Columns 43 through 49

 -0.0033 + 0.0142i   0.0017 + 0.0102i   0.0179 + 0.0093i   0.0209 + 0.0193i   0.0031 + 0.0096i  -0.0164 - 0.0113i  -0.0127 - 0.0183i

Columns 50 through 56

  0.0046 - 0.0168i   0.0074 - 0.0068i  -0.0042 + 0.0163i  -0.0178 + 0.0140i  -0.0397 - 0.0316i  -0.0598 - 0.0441i  -0.0432 + 0.0260i

Columns 57 through 63

  0.0005 + 0.0842i   0.0167 + 0.0393i   0.0000 - 0.0387i  -0.0041 - 0.0488i   0.0065 - 0.0199i  -0.0006 - 0.0165i  -0.0083 - 0.0172i

Columns 64 through 70

  0.0190 + 0.0097i   0.0510 + 0.0326i   0.0338 + 0.0255i  -0.0162 + 0.0034i  -0.0371 - 0.0277i  -0.0137 - 0.0579i   0.0103 - 0.0426i
```

Table 13: PAPR reduction in matrix form

5.2.8 Processing and reception of one DL sub frame – Transmitter Side

In this part, I generate PHY layer samples of the 3GPP E-UTRA Rel 8 downlink sub frame, normal CP or extended CP. A LTE sub frame time domain signal for our simulation (Figure 12).

In figure 14, we can see that the LTE sub frame has random values in time domain. The Y-axis denotes the amplitude of the signal. Now, figure 12 shows the resources per OFDM symbol and the corresponding time domain OFDM symbol.
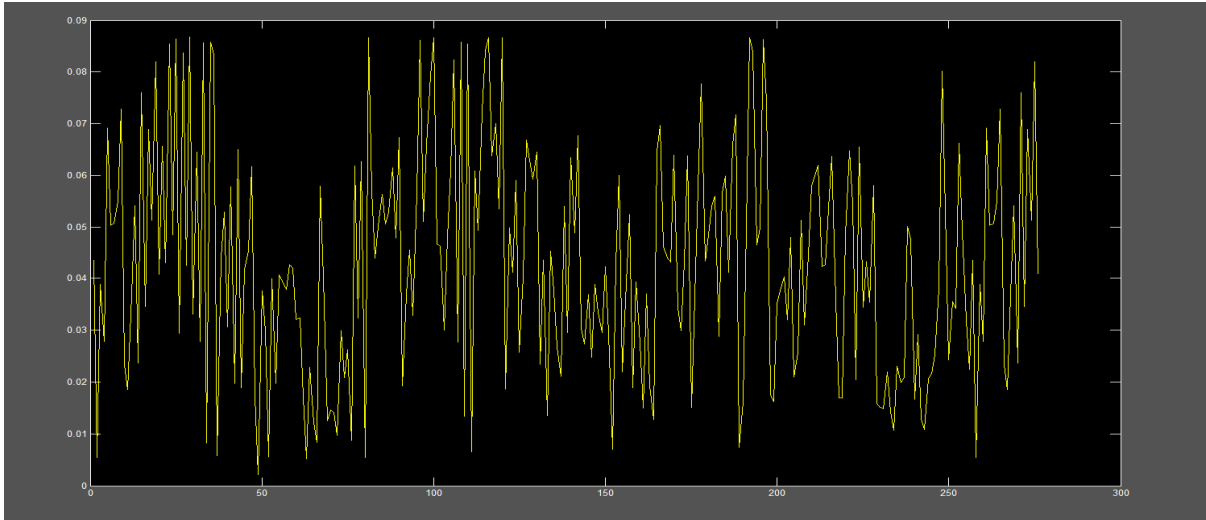
Figure 14: A LTE sub frame time domain signal

In figure 15, the first part shows the resource elements of the signal before the OFDM modulation. The second and third part show the signal in time and frequency domain. The figure illustrates the concept of an OFDM signal and the inter-relationship between the frequency and time domains. In the frequency domain, multiple adjacent tones or subcarriers are each independently modulated with complex data. Then in the time domain, guard intervals are inserted between each of the symbols to prevent inter-symbol interference at the receiver caused by multi-path delay spread in the radio channel.
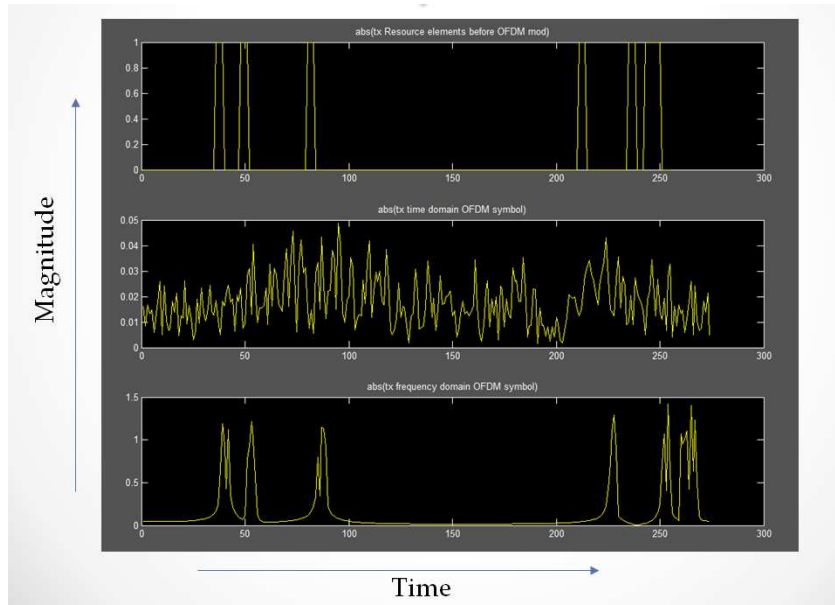
Figure 15: Resources per OFDM symbol (Time domain) – Transmitter Side

5.2.9 Processing and reception of one DL sub frame – Receiver Side

Here, we simulate the received PHY layer bit streams of the 3GPP E-UTRA Rel 8 downlink sub frame, normal CP or extended CP and performed OFDMA demodulation to get bit stream of each transmitted information.

Here are the sample parameters we set in the LTE PHY LAB:

numSubframe = 1

FFTsize = 128

numsPRB = [1 2]

N_cell_ID = Physical layer cell ID (0 – 503) = 0

PHICHtype = normal - 0 (one symbol mapping) or extended - 1 (3 symbols mapping) = 0

CPtype = 0

nF = Radio frame number = 0

Ng = detemine number of PHICH groups {1/6,1/2,1,2} = 1/6

modOrder = modulation order = 4

SNR = signal to noise ratio = 30

txSCHsize = transmitted SCH size = 10

Figure 16 represents the resources per OFDM symbol and the corresponding time domain OFDM symbol after simulation.

In figure 16, we can see that at the receiver, an FFT is performed on the OFDM symbols to recover the original data bits in time domain. As the figure illustrates, the frequency domain OFDM symbol has very low amplitude and same as for the transmitter resource elements.
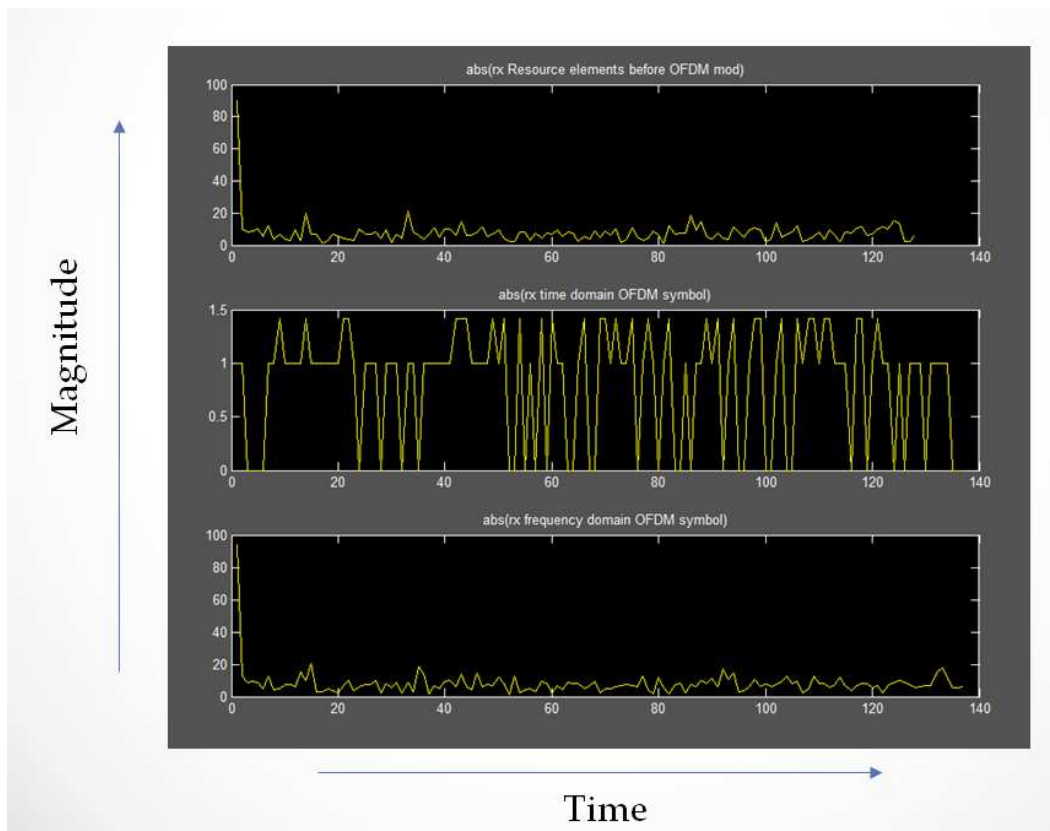
Figure 16: Resources per OFDM symbol (Time domain) – Receiver Side

The scatter plot of every received OFDM symbol can be shown in figure 17.
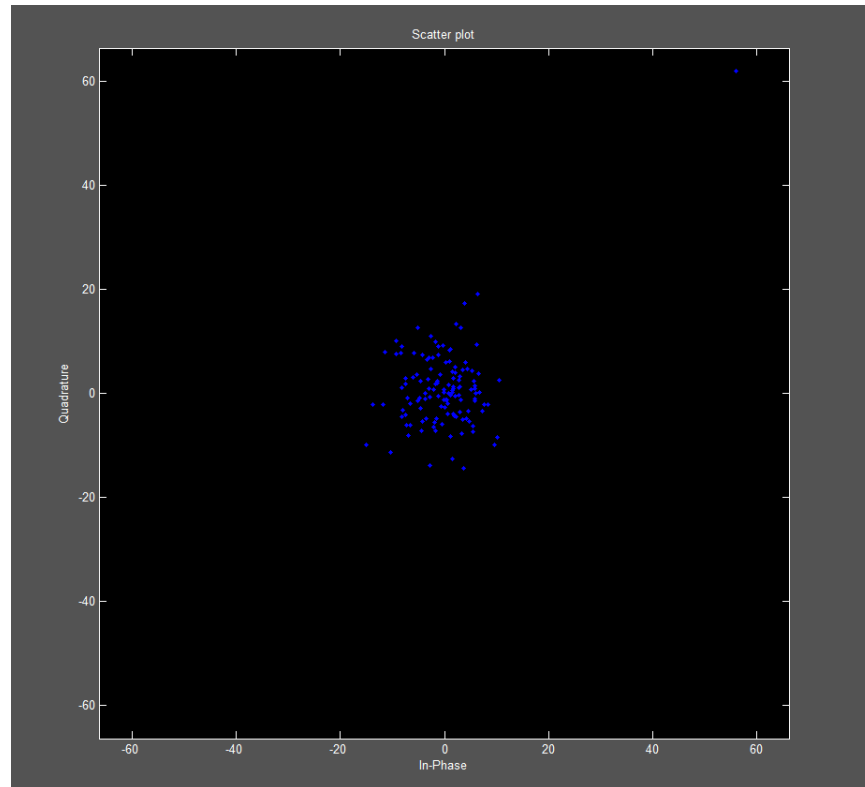
Figure 17: OFDM symbol constellation

In the figure 17, we can see that the input bits are grouped and mapped to source data symbols that are a complex number representing the modulation constellation point. For example, the BPSK or QAM symbols that would be present in a single subcarrier system. These complex source symbols are treated by the transmitter as though they are in the frequency-domain and are the inputs to an IFFT block that transforms the data into the time-domain.

5.2.10   Channel estimation for control and data channels

For performs channel estimation in downlink, we followed these algorithm steps [35,36]:

   - Estimate channel only for pilot signals arranged in a number of OFDMA symbols

- Estimate channel in frequency domain for the remaining sub-carriers for OFDMA symbols previously taken. The linear interpolation is used

- Estimate channel in time domain for all OFDMA symbols in resource grid. The linear (default), piecewise constant interpolation method could be used.

We got the below result for our channel estimation simulation part (Only column 1 to 14 of 512 has been shown here):

Table 14: Simulated matrix data after Channel Estimation

According to the simulated result, the estimated channel only for pilot signals arranged in a number of OFDMA symbols (red square). This estimates channel in frequency domain for the remaining sub-carriers for OFDMA symbols previously taken and in time domain for all OFDMA symbols in resource grid.

These are values we set for the parameters in LTE PHY LAB to see the simulated results for channel estimation:

FFTsize = size of the FFT used in OFDMA modulation = 128

43

numOFDMSym = 14

CPtype = measured CP type = 0

N_cell_ID = Physical layer cell ID (0 - 503) = 2

numPort = number of antenna port (0-3) = 0

numSubframe = subframe number (0 - 9) = 0

numAntennas = number of antennas used for transmission [Tx, Rx] = [1 1]

idxAntenna = number of mapping antenna = 1

nF = radio frame number (0 - ...) = 0

METHOD = interpolation method used in algorithms:

- 'linear'

- 'piecewise constant'

- 'averaged'

- 'pilot_averaged'

if METHOD is [] than default interpolation method will be used. It works only for MISO, the numAntennas(2): Rx is ignored = []

5.2.11   Simulation results of LSE and performances comparison with MMSE

To simulate the LSE algorithm, we set some values for the desired parameters:

N = Total number of sub channels = 256

P = Total number of Pilots = 256/8

S = Total number of data sub channels = N-P

GI = Guard interval length = N/4

M = Modulation = 2

pilotInterval = pilot position interval = 8

L = Channel length = 16

nIteration = Number of iteration in each evaluation = 500

SNR_V = signal to noise ratio vector in dB = [0:3:27]

After setting the above parameters in MATLAB, we got simulated results in figure 18.
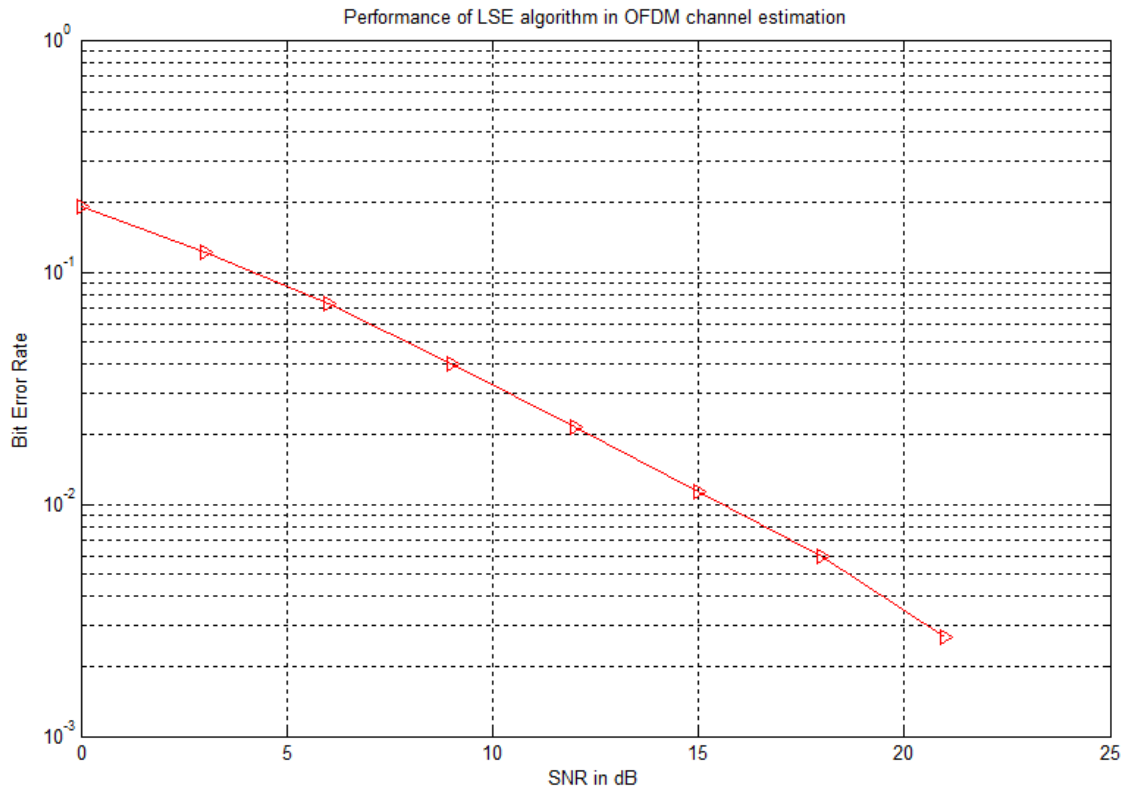

Figure 18: Performance of LSE algorithm in OFDM Channel Estimation

The figure 18 provides the BER vs SNR graph for LSE channel estimation algorithm. In this simulation, I used 2x2 MIMO-OFDM system and pilots are inserted among data for initial LS extimation. The channel between transmitter and receiver is according to multipath Rayleigh fading channel. Here, I used channel bandwidth 3.0 MHz. According to the graph, we can understand that the SNR increased in a greater extent with simulatenous decrease in bit error rate.

As LSE is comparatively simple algorithm, we investigate the performance of MMSE here. Below is the comparison of the performances of the LS and the MMSE channel estimators for a 64 sub carrier OFDM system based on the parameter of Symbol Error Rate.

According to the figure 19, the Least Square Error (LSE) and Minimum Mean Square Error (MMSE) alogirithms are used to time varying analysis of channel estimation methods in OFDM. We can see that the MMSE looks worse than LSE in this graph. The bit error rate is affected by the signal to noise ratio (SNR) value. As the SNR value increases the bit error rate decreases but data rate increases.
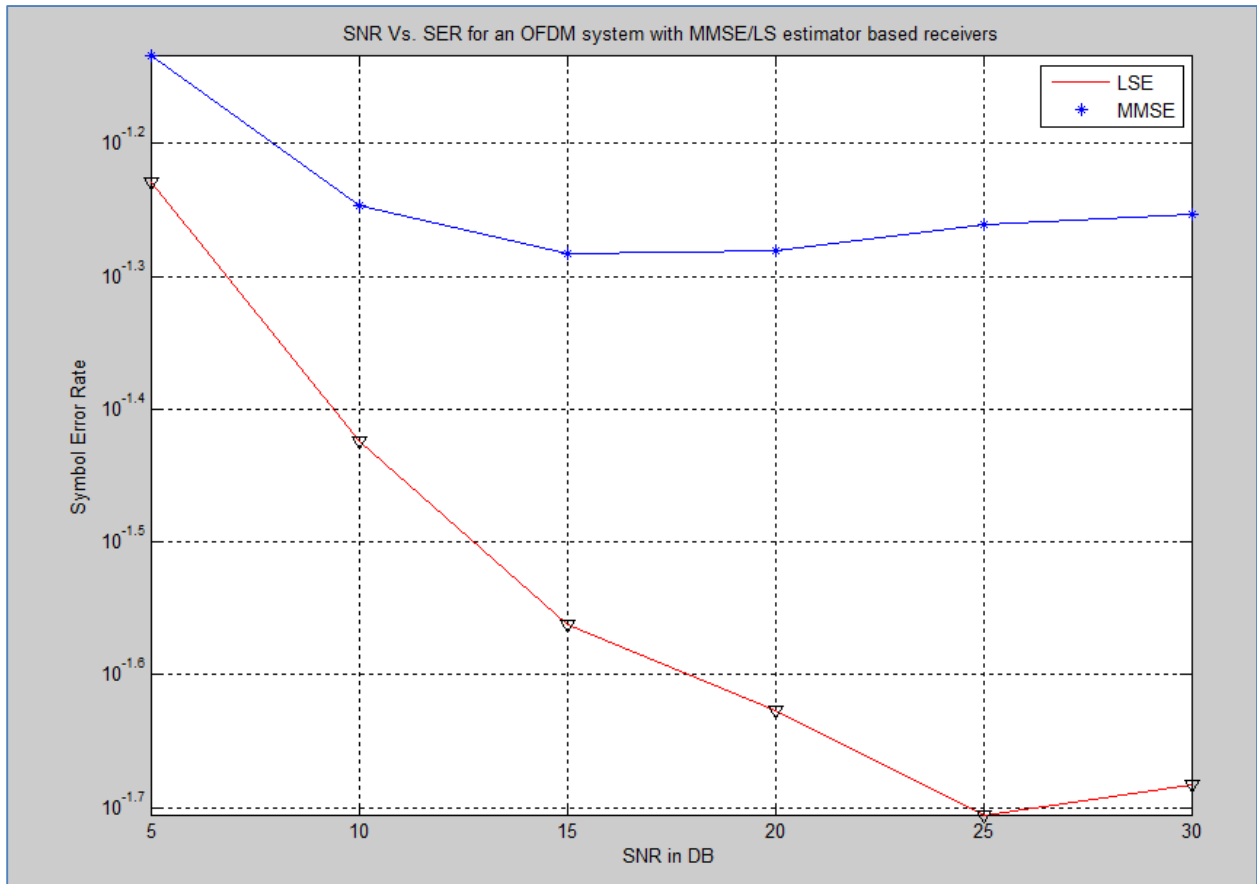

Figure 19: SNR Vs. SER for an OFDM symbol with MMSE/LS estimator based receivers

Now, from the simulated result, we can understand that larger the SNR value higher accuracy of estimation will be achieved. So, the relation between SNR and BER for both LSE and MMSE channel estimation is inversely proportional. However, the performance of LSE looks better than MMSE.

CHAPTER 6

CONCLUSIONS AND FUTURE WORK

The main purpose of this thesis work is to evaluate different channel estimation methods for LTE downlink systems under various channel conditions. We have presented the experimental results by means of simulations. LS estimator is computationally simple and efficient for high SNR values. For higher constellation mapping at high mobile speeds, its performance would be degraded. MMSE estimator could be a better solution for higher modulation schemes and large delay spreads even though it is computationally complex. The thesis work findings can be summarized in the following steps:

- Basic understanding of LTE and its physical layers. Special emphasis on LTE downlink frame structure and in time domain and frequency domain, reference symbols structure and multiple antenna techniques for LTE.

- Link and frame level simulation has been done for MIMO-OFDM system.

- Different kinds of fading channel considered for channel estimation.

- Performance comparison has been done for LSE and MMSE algorithm.

- Detailed channel estimation simulation done in terms of matrix data in LTE PHY LAB.

The future work could be described as below:

- Channel estimation for Uplink could be investigated for different channel conditions

- There are some other complex channel estimation algorithm are available now which are still need to be simulated and implemented.

- Performance analysis of different uplink and downlink channel estimation algorithms for MU-MIMO (2X2, 4X4)

- Error performance as a function Rayleigh Fading

APPENDIX

Please contact IS-Wireless Inc. for codes and materials. Here is the contact info:

IS-Wireless Inc.

Pulawska Plaza

Ul. Pulawska 45b

05-500 Piaseczno/near Warsaw, Poland

Email: info@is-wireless.com

Tel: +48 22 213 8297

Fax: +48 22 213 8298

REFERENCES

[1]   A. S. Shaikh and K. C. Kumar, "Performance Evaluation of LTE Physical Layer Using SC-FDMA & OFDMA," 2010.

[2]   (13th July, 2014). *LTE PHY LAB, IS-Wireless Inc*. Available: http://is-wireless.com

[3]   (13th July, 2014). *Wireless Technology Evolution*. Available: http://appleinsider.com

[4]   S. Saleem, Qamar-ul-Islam, W. Aziz, and A. Basit, "Performance Evaluation of Linear Channel Estimation Algorithms for MIMO-OFDM in LTE-Advanced," *International Journal of Electrical & Computer Sciences,* 2011.

[5]   (13th July, 2014). *Channel access method*. Available: http://en.wikipedia.org/wiki/Channel_access_method

[6]   (14th July, 2014). *LTE Frequency band allocations*. Available: http://www.telecom-cloud.net

[7]   C. Lélé, J. P. Javaudin, R. Legouable, A. Skrzypczak, and P. Siohan, "Channel estimation methods for preamble-based OFDM/OQAM modulations," *European Transactions on Telecommunications,* vol. 19, pp. 741-750, 2008.

[8]   (13th July, 2014). *LTE frame structure*. Available: http://www.radio-electronics.com

[9]   L. J. Cimini, "Analysis and Simulation of a Digital Mobile Channel Using Orthogonal Frequency Division Multiplexing," *Communications, IEEE Transactions on,* vol. 33, pp. 665-675, 1985.

[10]   R. R. G. Americas, "HSPA to LTE-Advanced: 3GPP Broadband Evolution to IMT-Advanced (4G) [White Paper]," 2009.

[11]   M. K. Ozdemir and H. Arslan, "Channel estimation for wireless ofdm systems," *Communications Surveys & Tutorials, IEEE,* vol. 9, pp. 18-48, 2007.

[12]   N. Larsson, "Analysis of channel estimation methods for OFDMA," 2006.

[13]   (14th   July,   2014).   *Additive   white   Gaussian   noise*.   Available:
         http://en.wikipedia.org/wiki/Additive_white_Gaussian_noise

[14]   S. Faruque, *Cellular Mobile Systems Engineering*: Artech House, Inc, 1996.

[15]   H. Holma and A. Toskala, *LTE for UMTS: OFDMA and SC-FDMA Based Radio Access*,
         2009.

[16]   L. S, "Channel Estimation and Prediction In UMTS LTE," Aalborg University, 2007.

[17]   G. M. Kebede and O. O. Paul, "Performance Evaluation of LTE Downlink with MIMO
         Techniques," 2010.

[18]   S. Pathak and H. Sharma, "Channel Estimation in OFDM Systems," *International
         Journal of Advanced Research in Computer Science and Software Engineering,* 2013.

[19]   (13th July, 2014). *LTE Resource Block*. Available: http://www.teletopix.org

[20]   (13th July, 2014). LTE Modulation Constellations. Available: http://m.eet.com/

[21]   S. Myung Jun, H. Jung-Su, R. Hee-Jin, and C. Hyung-Jin, "A frequency synchronization
         method for 3GPP LTE OFDMA system in TDD mode," in *Communications and
         Information Technology, 2009. ISCIT 2009. 9th International Symposium on*, 2009, pp.
         864-868.

[22]   M. Ibnkahla, *Signal Processing for Mobile Communications Hand book*: CRC Press,
         2005.

[20]   (13th July, 2014). FDD LTE Frequency band allocations. Available: http://www.telecom-
         cloud.net

[21]   C. Johnson, *Long Term Evolution in Bullets*, 2010.

[22]   M. B. Sen, "Channel Estimation Techniques For Single And Multiple Transmit Antenna
         Orthogonal Frequency Division Multiplexing (OFDM) Systems," 2005.

[23]   J. J. van de Beek, O. Edfors, M. Sandell, S. K. Wilson, and P. Ola Borjesson, "On channel estimation in OFDM systems," in *Vehicular Technology Conference, 1995 IEEE 45th*, 1995, pp. 815-819 vol.2.

[24]   A. Mehmodd and W. A. Cheema, "Channel Estimation for LTE Downlink," 2009.

[25]   A. Ancora, C. Bona, and D. T. M. Slock, "Down-Sampled Impulse Response Least-Squares Channel Estimation for LTE OFDMA," in *Acoustics, Speech and Signal Processing, 2007. ICASSP 2007. IEEE International Conference on*, 2007, pp. III-293-III-296.

[26]   T. V. 3GPP, "Physical Layer Aspects for Evolved Universal Terrestrial Radio Access (UTRA), Release 7," 2006.

[27]   *Technical Specifications Guide*. LTE PHY LAB v.1.2.

[28]   D. Mannai, "Modeling and Simulation of Scheduling Algorithms in LTE Networks," 2012.

[29]   J. Pierzchlewski and T. Larsen. (2012, 13th July, 2014). *LTE Downlink Transmitter Simulation Using MATLAB*. Available: http://www.microwavejournal.com

[30]   F. Rezaei, "A Comprehensive Analysis of LTE Physical Layer," 2010.

[31]   H. Die, Y. Luxi, S. Yuhui, and H. Lianghua, "Optimal pilot sequence design for channel estimation in MIMO OFDM systems," *Communications Letters, IEEE,* vol. 10, pp. 1-3, 2006.

[32]   L. Zhang, "Network Capacity, Coverage Estimation and Frequency Planning of 3GPP Long Term Evolution," 2010.

[33]   S. Changyong, R. W. Heath, and E. J. Powers, "Blind Channel Estimation for MIMO-OFDM Systems," *Vehicular Technology, IEEE Transactions on,* vol. 56, pp. 670-685, 2007.

[34] M. Dhawan, "Bandwidth Efficient Coded Modulation for Broadband communication," UND, 2011.

[35] L. F. M. Reya, "4G Technology Features and Evolution towards IMT-Advanced," 2010.

[36] D. Martin-Sacristan, J. Cabrejas, D. Calabuig, and J. F. Monserrat, "MAC Layer Performance of Different Channel Estimation Techniques in UTRAN LTE Downlink," in *Vehicular Technology Conference, 2009. VTC Spring 2009. IEEE 69th*, 2009, pp. 1-5.